

# In.To. COVID-19 Socio-epidemiological Co-causality

**Elroy Galbraith**

Hokkaido University

**Matteo Convertino** (✉ [matteo@ist.hokudai.ac.jp](mailto:matteo@ist.hokudai.ac.jp))

Tsinghua University <https://orcid.org/0000-0001-7003-7587>

**Jie Li**

Hokkaido University

**Victor Del-Rio Vilas**

WHO

---

## Article

### Keywords:

**Posted Date:** June 1st, 2021

**DOI:** <https://doi.org/10.21203/rs.3.rs-571447/v1>

**License:**   This work is licensed under a Creative Commons Attribution 4.0 International License.

[Read Full License](#)

---

# In.To. COVID-19 Socio-epidemiological Co-causality

Elroy Galbraith<sup>a</sup>, Matteo Convertino<sup>a,b\*</sup>, Jie Li<sup>a</sup>, Victor Del  
Rio-Vilas<sup>c</sup>

<sup>a</sup> Nexus Group, Faculty and Graduate School of Information Science and  
Technology, Hokkaido University, Sapporo, JP

<sup>b</sup> Institute of Environment and Ecology, Tsinghua Shenzhen International  
Graduate School, Tsinghua University, Shenzhen, China

<sup>c</sup> SEARO/WHO, New Delhi, India

May 26, 2021

*Corresponding author:* \* M. Convertino, Tsinghua Shenzhen International Graduate  
School, University Town of Shenzhen, Tsinghua Park, Nanshan District, Shenzhen 518055  
P.R. China, email: matconv.uni@gmail.com

*Keywords:* infodemiology, infoveillance, positivity, healthcare pressure, misinformation

## Abstract

Social media can forecast disease dynamics, but infoveillance remains focused on infection spread, with little consideration of media content reliability and its relationship to behavior-driven epidemiological outcomes. Sentiment-encoded social media indicators have been poorly developed for expressed text to forecast healthcare pressure and infer population risk perception patterns.

Here we introduce Infodemic Tomography (InTo) as the first web-based interactive infoveillance cybertechnology that forecasts and visualizes spatio-temporal sentiments and healthcare pressure as a function of social media positivity (i.e., Twitter here), considering both epidemic information and potential misinformation. Information spread is measured on volume and retweets and the Value of Misinformation (VoMi) is introduced as the impact on forecast accuracy where misinformation has the highest dissimilarity in information dynamics. We validate InTo for COVID-19 in New Delhi and three other SE Asian cities. We forecast weekly hospitalization and cases using ARIMA models and interpolate spatial hospitalization using geostatistical kriging on inferred risk perception curves between tweet positivity and epidemiological outcomes. Geospatial tweet positivity tracks accurately  $\sim 60\%$  of hospitalizations and forecasts hospitalization risk hotspots along risk aversion gradients. VoMi is higher for risk-prone areas and time periods, where misinformation has the highest predictability, with high incidence and positivity manifesting popularity-seeking social dynamics.

Hospitalization gradients, VoMi, effective healthcare pressure and spatial model-data gaps can be used to predict hospitalization fluxes, misinformation, capacity gaps and surveillance uncertainty. Thus, InTo is a participatory instrument to better prepare and respond to public health crises by extracting and combining salient epidemiological and social surveillance at any desired space-time scale.

41       *“Not everything that can be counted counts*  
42       *and not everything that counts can be counted”’*  
43       Albert Einstein  
44

## 45   1   Introduction

### 46   1.1   COVID-19 and Infeveillance

47   The spread and magnitude of COVID-19 is reflected in social media production and senti-  
48   ments with the lowest ever recorded trend in population positivity (see the Hedonometer at  
49   [https://hedonometer.org/timeseries/en\\_all/](https://hedonometer.org/timeseries/en_all/)). Not only are social media messages the  
50   saddest they have been since happiness monitoring began (see [Dodds et al. \(2011\)](#)), but the  
51   volume of misinformation has grown exponentially ([Gallotti et al., 2020](#); [Islam et al., 2020](#)).  
52   These observations provide evidence of the relevance of socio-technological systems like so-  
53   cial media to predict epidemiology. Empirical evidence for many diseases before COVID-19  
54   and previous analytical findings made clear the linkage between risk perception and infection  
55   patterns ([Maharaj and Kleczkowski, 2012a](#)); thus, highlighting the co-causality of social and  
56   epidemiological information beyond their predictability.

57   Aware of these linkages, global response to COVID-19 by health authorities includes risk  
58   communication messages, e.g. on increasing social distancing and using masks to reduce inter-  
59   person transmission. Similarly, messages on enhancing early identification, isolation and care  
60   for patients all in a bid to “flatten the curve” shed light on the importance of surveillance  
61   and public health capacities ([Thunström et al., 2020](#)). The search for social surveillance  
62   tools that could help public health officials to monitor, forecast, plan, evaluate and prepare  
63   for public health demand started well before COVID, e.g. with seasonal influenza in USA  
64   coupled to predictive multimodeling (see [Paul et al. \(2014\)](#), [Santillana et al. \(2015\)](#) and  
65   [McGowan et al. \(2019\)](#)), due to the recognition of the limitations – e.g. delays, misreporting  
66   – of traditional epidemiological surveillance systems. In analogy, social media signals are  
67   also used to forecast, a priori or in near real-time, extreme environmental phenomena such  
68   as earthquakes ([Sakaki et al., 2010](#)), which highlights the relevance of temporal and spatial  
69   social media for surveillance.

70   Concurrently to the spread of COVID-19 epidemic, health authorities are combating an  
71   infodemic, strictly defined as the rapid exponential increase in the volume of potentially

misleading information about an event (WHO et al., 2020). Misinformation, considered as objectively false or inaccurate information, is of difficult detection and classification because it is highly affected by perception bias. Misinformation can tangibly and negatively impact response strategies and health-seeking behaviors (Ung, 2020; Otto and Eichstaedt, 2018; Maharaj and Kleczkowski, 2012b) which may lead to increased infections and hospitalization. Against this background, infodemiology and infoveillance (Eysenbach, 2009) emerge as a strong public health response to the COVID-19 pandemic. Infodemiology applies principles of epidemiology to the study of emergence and spread of misinformation, while infoveillance applies information technology solutions to the monitoring and forecast of disease spread as well as visualization of salient outputs (from main patterns to predictions). Prior to COVID-19, scientists have been able to use internet dynamics and message sentiments to monitor public health related phenomena and forecast disease spread (Ginsberg et al., 2009; Eysenbach, 2009; Bragazzi, 2013; Eichstaedt et al., 2015; Santillana et al., 2015; Radin and Sciascia, 2017). However, no model or information system used social media sentiments to forecast sentiments (as continuous variables versus categorical emotions) and healthcare pressure (cases and hospitalization) together, over space and time; epidemiology and information patterns have always been disjoined, yet neglecting the ability to quantify the effective impact of information – and misinformation alike – on populations.

## 1.2 Information-Prediction Nexus

A different perspective on public health forecasting is brought by proposing an assumption-free minimalist model that is focused on patterns rather than processes of the phenomena considered. The employed information-theoretic models (perfectly fitting the general aims of infoveillance) are using the necessary and sufficient social data as sentinels of change, coupled to epidemiological information, to maximize prediction accuracy for the patterns investigated. Information theoretic models like the one proposed here are the least biased models (mechanisms-free) for capturing which set of information is relevant for predicting patterns. Other underlying causal factors, such as local language and socio-environmental factors of the population considered, are certainly important in the domain of physical reality but not in the information domain of predictions. Therefore, the focus is on predictive causality rather than true causality (Li and Convertino, 2020); a principle that, however, should be associated to any model considering the fundamental reality of any model as a microscope of reality rather than its utopian replica.

105 With the aforementioned reasoning in mind, social and epidemiological processes (and yet  
 106 data about them) are linked by information and misinformation that is revealing patterns  
 107 of people behavior in terms of sentiments (informative of risk perception) and cases, respec-  
 108 tively. Additionally, strong predictive causality in process-related variables has been shown to  
 109 coincide with physical causality; yet, computation that screens and weights information can  
 110 be used to infer co-causality between two signals robustly, without imposing any assumption  
 111 a priori on model structure.

112 In the current COVID-19 context, we are interested in knowing whether modern social  
 113 media are predictive of explosive epidemics, and more precisely which social chatter features  
 114 are the most predictive of epidemiological patterns. Moreover, whether social chatter features  
 115 can be accurately used as early warning predictors of risk before cases occur, and how early  
 116 can forecasts be made. Motivated by these questions we developed InTo as an exploratory tool  
 117 to quantify how much perceived risk inferred from social chatter in advance was predictive of  
 118 actual observed risk in cases and extreme cases (or hospitalization) reported by official public  
 119 health surveillance. This modus operandi and modern infoveillance tool, beyond assessing  
 120 how much waves in socio- and health-scapes copredict each other via joint “infoscapes”, can  
 121 validate classical surveillance systems (which provide data that are byproducts of behavioral  
 122 models, oftentimes affected by strong bias) considering the temporal gap between model and  
 123 data for multiple surveillance criteria (Vilas et al., 2017). Theoretically, the smaller the gap  
 124 over time the higher the surveillance accuracy.

### 125 1.3 InTo: Infodemic Tomography

126 Infodemic Tomography (In.To. or InTo hereafter) was developed as a cybertechnology to  
 127 forecast one week in advance COVID-19 related cases, hospitalizations, population positiv-  
 128 ity, misinformation impact and spreading, healthcare satisfaction and space-time surveillance  
 129 uncertainty by leveraging geospatial Tweets and epidemiological data in New Delhi. InTo  
 130 analyzes and visualizes “tomograms” or snapshots of epidemiological and information dy-  
 131 namics for the selected geographies. Thus, InTo is proposed as a Digital Health platform  
 132 for Participatory, Predictive, Personalized, Preventive and Precise Health (“P5”), that is an  
 133 “upgrade” with respect to the “P4” purview of health, such as in Alonso et al. (2019), via  
 134 the *precise* identification and provision of systemic health-related information to individuals  
 135 and populations alike. Weather forecasting is the general epitome of InTo considering its  
 136 focus on predicting patterns of healthcare pressure as a function of dynamically updated  
 137 information; thus the InTo dashboard is ideally like an App visualizing the most updated

138 weather forecasts.

139 Previous efforts have focused on internet-based social media for incidence surveillance and  
140 outbreak forecasting (Barros et al., 2020). Some of these efforts incorporated hospital visit  
141 data in their models (Ram et al., 2015) but none of them coupled social and epidemiological or  
142 healthcare information together. InTo goes beyond temporal incidence predictions because it  
143 aims to investigate changes in socio-epi patterns over time and space and the value of spatial  
144 social chatter by dynamically calibrating the model as data from social and epidemiological  
145 surveillance is updated. In this optic and in relation to the early forecasting nature of InTo,  
146 the predicted hospitalization is informative of people potentially in need of hospitalization  
147 one week in advance. Gradients of hospitalization over space are indicative of patient hospital  
148 loads. In an hydroclimatological analogy, gradients of healthcare pressure are like gradients  
149 in atmospheric pressure dictating where ill people/rain will likely flow, and exceedance of  
150 pressure over healthcare capacity are like floods.

151 Considering previous efforts, InTo is the first cyberinfrastructure to forecast COVID-19  
152 specific healthcare pressure (as difference between point- and city-scale predicted cases and  
153 hospitalization) as a function of text positivity where the latter is a variable quantifying  
154 potential happiness in words shared via social media, i.e. Twitter in this context. Although  
155 InTo is not the first to examine the relationship between Twitter sentiments and diseases,  
156 previous efforts were based on extracting few categorical emotions or using volume of social  
157 media entries as predictive functions (Haghighi et al., 2017; Roccetti et al., 2017; Eichstaedt  
158 et al., 2015; Wilson et al., 2014b). InTo instead is the first effort, set of models and par-  
159 ticipatory dashboard to use quantitative measures of continuous sentiments (associated also  
160 to potential misinformation) as positivity to forecast healthcare pressure over space and one  
161 week in advance, coupled to the evaluation of those forecasts within an information-theoretic  
162 framework.

163 In the development of InTo we chose to call happiness, introduced by Dodds et al. (2011).  
164 as positivity because it is semantically a more general word that does not imply happiness  
165 (strict sensu) and relates more effectively to risk behavioral patterns (related to the objective  
166 relative risk conditional to the geographical area considered), at least conceptually. Gradi-  
167 ents in positivity as a function of cases or hospitalizations define risk perception patterns on  
168 which predictive models are calibrated to produce forecasts. Linear predictive models are  
169 used to perform infection and hospitalization predictions whose predictive power is tested  
170 via non-linear predictability indicators (i.e., Transfer Entropy measuring the time delayed  
171 uncertainty reduction between positivity and epidemiological variables, as discussed in the

Material, Methods and Implementation section). These indicators are based on probability distribution functions of the variables of interest and yet they consider uncertainty distribution attributable to other unexplained uncertainty sources. In this broad framework, properly calibrated positivity fluctuations are good sentinels of relative hospitalization risks – and yet good predictors – as much as heat index fluctuations are good sentinels of extreme temperature hospitalization (Liu et al., 2018) to mention an analogous public health effort focused on detecting optimal indicators for risk communication.

The paper presents the workflow in Fig. 1 and implementation of InTo by using the case of New Delhi to demonstrate its applicability and utility for COVID-19 and in general for any disease. Part of the demonstration includes results of validation exercises conducted to evaluate the developed models. We then discuss limitations of InTo, especially in terms of data availability, representativeness and model complexity. We conclude by outlining future work for InTo.

## 2 Case Study Results

Here we present InTo as an infoveillance system for the case of New Delhi during the COVID-19 pandemic between April and July 2020. New Delhi is chosen as the prototypical city to display because of its highly coupled social and epidemiological dynamics as empirically found from data. In InTo, once the user selects their city of interest, results of analyses are displayed as a series of visualizations divided into four main sections corresponding to tabs of the dashboard: Healthcare Pressure, Emotions and Misinformation, Predictability and Tweet Spread (Figs. 2-6).

### 2.1 Healthcare Pressure

The layout of the Healthcare Pressure tab is displayed in Figures 2 and 3. In New Delhi between April 15 and July 30 public positivity captured from COVID-19 related tweets ranged between 5.6 and 6.0 with a slight downtrend from 5.85 at the beginning of the period to 5.73 at the end. Meanwhile, there was a trend reversal in new cases and the cumulative hospitalization, with new hospitalizations showing an increase in the magnitude of fluctuations closer to the end of the period. Positivity was at its lowest in June when cumulative hospitalizations was at its highest but positivity was highest in July when hospitalization began to increase



again. By using the linear relationship between hospitalization and positivity (see ARIMA model at Eq. 5.3), on July 30th we predicted next week's hospitalization to decrease by 381 hospitalizations (i.e. new hospitalizations displayed in the left plot of the dashboard), and cases to increase by 549. Cumulative hospitalization and cases were about 20,000 and 1500 on July 30th (left plots in the dashboard). In Figure 8 we present the results of using positivity from all tweets to forecast daily new hospitalization and daily new cases. Spatial forecasts related to misinformation are not shown spatially. Considering the spatial distribution of positivity and hospitalization in the two weeks before forecasting, via geostatistical kriging (Eqs. 5.4-5.7) we forecasted two large clusters of hospitalization in the North-West and South-East and a smaller cluster in the center of New Delhi. In the high healthcare pressure areas colored in red, we estimated that there would be almost 200 new individuals in need of hospitalization (see color bar in the dashboard screen). These are calculated via the geokriging model (Eqs. 5.4-5.7).

In order to highlight spatial gradients of hospitalization (meaningful of potential mobility gradients of people in need of hospitalization mediated by the presence of healthcare facilities; see Fig. 3) we decided to visualize healthcare pressure  $H_{P_i}$ , that is calculated as the difference between locally expected hospitalization and average hospitalization (Eq. 5.8). The numbers displayed on the top of the dashboard refer to expected new hospitalization and hospitalization change from ARIMA (Eq. 5.3) for the entire city.  $H_{P_i}$  is visualized in a green-red color shade (where red is for the highest  $H_{P_i}$ ) for  $M$  randomly generated points (10,000) over the city which are interpolated using the geokriging using the semivariogram of positivity. The area encompassed by each point is in the range 0.5-1.0  $km^2$ , depending on the spacing between points; thus, our forecasts provide a high spatial resolution compared to surveillance systems. The 200 newly predicted hospitalizations displayed in the dashboard constitute the peaks above the average (or the maximum healthcare pressure) in the entire city. The average is  $\sim 12$  according to the geokriging, and that corresponds to the ARIMA average shown on the top of the dashboard (see Fig 2). The average new hospitalizations matches matches very closely the observed hospitalizations from surveillance (i.e. 11). Note that  $\sim 200$  hospitalizations are for few areas in the city and these extreme values are well above the average value for the period considered. The total number of hospitalization in a selected area can be calculate as sum of new hospitalizations for all the points in that area.

Considering these results for the week displayed, hospital managers may wish to focus their attention to the North-West and South-East areas of New Delhi (lacking healthcare capacity as displayed by the geolocated and visualized hospitals in Fig. 2) where individuals in

need of hospitalizations are potentially looking for treatment in other areas, and thus establishing hospitalization fluxes. Positivity fluctuates around the same city-specific mean, while cumulative hospitalization grows exponentially over the course of the epidemic. Theoretical Gaussian and exponential variograms were the best fit for positivity and for cumulative hospitalization, as expected considering their time dynamics (left plots in the dashboard in Fig. 2).

Figure 3 shows a snapshot of forecasts in mid July 2020 when very distinct clusters of hospitalizations are identified. The figure serves to highlight how gradients in hospitalization pressure are meaningful of potential mobility of people in need of hospitalization and this expected mobility is dependent on local healthcare capacity that determines the ability to treat patients in need. Effective healthcare pressure can be calculated by considering local healthcare capacity (as number of beds, ventilators or other resources needed to treat patients) and expected hospitalization.

## 2.2 Emotions, Top Words, and Misinformation

Emotions, from emotion inference algorithms (see Section 5.3), are extracted from the systemic information (all the tweets), misinformation tweets, and healthcare-specific tweets throughout the epidemic. Tweets for each category are reported on the right of the tab (Fig. 4) and some of these tweets can be directly reported to InTo as misinformation by social media (Twitter) users. Below we report results that can be inferred by using InTo, such as specific events, word pairs, users and associated emotions. When considering all tweets, the dominant emotion over time was trust, followed by fear and anticipation; joy and sadness were the next most frequent; surprise and disgust were expressed the least. This distribution was observed for the subset of tweets related to misinformation as well, however there was one day, on June 10th, when these tweets expressed more fear than they did trust. As for tweets related to healthcare, trust was usually most expressed, but it was not as dominant as in the case of all tweets or misinformation. Furthermore, sadness seemed to be expressed much more among these tweets, especially in early June. On June 10, the saddest day considering healthcare tweets, the most retweeted tweet was from a user who felt abandoned and helpless after struggling to help his sister and her two small children after her husband had died from the disease. Similar tragic tweets reported the lowest positivity. The most frequent healthcare tweets were also about the lack of beds, inability of hospitals to provide proper service, and the possibility of public health officials to hide the true number of cases. Worryingly, users were also taking the opportunity to request blood donors via Twitter. On

July 22nd 2020, the most frequent pairs of words referenced were about “public health advice” and “self-quarantine at home”. A review of the raw tweets showed that many of the tweets were actually tweets of news articles made by organizations rather than individuals. Such tweets tended to be “neutral” in their positivity (i.e. centered around 5 without an increasing or decreasing trend), with values ranging between 4 and 6. This emphasizes the tendency of organizations, versus individuals, in manifesting risk-neutral perception patterns corresponding to average values of positivity.

## 2.3 Predictability and Forecasting

Predictability indices (Section 5.5) are reported in Figure 5 for both cases and hospitalizations as values over 100; yet, percentage changes are easily quantifiable. The risk index confirmed that cases were declining over time, despite momentary increases. This index showed the same trend for the full tweet and misinformation datasets because it is based on the same data (the time series are reported twice to compare infection and hospitalization trends against systemic information and misinformation indices). A model-based risk indicator can be calculated to visualize the risk in terms of predicted values rather than data only.

Between May and June tweet positivity was under-predicting cases but then began to over-predict cases in July. Tweet positivity and cases showed a mostly moderately negative correlation (mean corr= -0.24). Although the value of the correlation was constant, suggesting a reliable model or stable dynamics, predictability was not stable until late June, when the predictability indicator became very small indicating lack of non-linearity, and thus implying high reliability in the linear forecasting of cases via the ARIMA model. All results suggest that tweet positivity from all downloaded tweets was most meaningful for forecasting the spatio-temporal spread in July, with relatively high uncertainty earlier. July has the highest correlation coefficient (in magnitude), lowest gap and non-linear predictability, as well as the lowest VoMi (Eq. 5.13). The subset of tweets related to misinformation showed a similarly negative though much weaker correlation with cases (mean corr = -0.01). This is concordant to the much higher non-linear predictability of misinformation manifesting the decreasing forecasting accuracy of ARIMA for this tweet subset.

When considering all tweets, the model mostly under-predicted hospitalizations, with its largest under-prediction occurring in late June after hospitalization became the largest in the end of May (bottom left plot of Fig. 5). The largest over-prediction was observed in late July after hospitalization risk became very large. Yet, very large spikes in risk seemed

301 to produce very large gaps in predictions. These large gaps are driven by misinformation  
 302 as shown by the VoMi assessment that is higher at the end of the monitored period. The  
 303 value of misinformation (Eq. 5.13) showed a gradual uptrend, indicating that tweets related  
 304 to misinformation were decreasing the forecasting accuracy (based on linear correlation) of  
 305 all tweets for cases and hospitalization as time progressed. Tweet positivity was mostly  
 306 negatively correlated with hospitalization but predictability was low, especially for hospital-  
 307 ization. This underlines the fact that there is more linearity between new hospitalization and  
 308 positivity than cases and positivity, and yet the ARIMA forecasts are more reliable for new  
 309 hospitalization. Despite this average result we observe that larger fluctuations in indicators  
 310 are seen for hospitalization than cases, likely underlying the necessity to include other pre-  
 311 dictors for extreme hospitalization events. Lastly, time series of indicators for all tweets and  
 312 misinformative tweets are quite similar due to the low detection of misinformation; nonethe-  
 313 less time-point values are different as manifested by VoMi because misinformation, although  
 314 small, exist and impact forecasts.

## 315 **2.4 Tweet Spread**

316 The Tweet Spread tab (Fig. 6) shows the volume of tweets and retweets, as well as their  
 317 positivity, for the systemic information and misinformation set. There were between 10,000  
 318 and 100,000 tweets per week related to COVID-19 in New Delhi. The volume of retweets was  
 319 much lower in comparison, not exceeding 10 retweets, and had positivity values approach  
 320 6 meaning they were more positive than the average neutral value of 5. Additionally, both  
 321 tweet volume, retweets and positivity are slowly decreasing over time which manifest the  
 322 lower COVID information production and decreasing positivity.

323 The number of misinformation tweets was the highest in the early days of the pandemic  
 324 descending relatively rapidly as time progressed. The retweet volume was very low com-  
 325 pared to the full tweet set (the difference is about three orders of magnitude) and most of  
 326 the popular misinformative tweets had low positivity. One of these popular misinformation  
 327 tweets called for the protection of citizens of different religions who were being implicated  
 328 and arrested on false charges. This tweet underlines the fact that misinformation is not nec-  
 329 essarily carrying deceiving information but also information about perceived wrong behavior  
 330 in populations. Thus, misinformation can capture more the dichotomy between common and  
 331 divergent groups in the area analyzed. The large difference in volume of all tweets ( $\sim 10^5$ ) and  
 332 misinformative tweets (that are less than  $10^3$ , two orders of magnitude less than all Tweets)  
 333 explains why time series dynamics of predictability indicators for the systemic information

334 and misinformation predictors (Fig. 5) is very similar but time point values are different.

335

## 336 2.5 Model Calibration and Validation

337 Results of the model validation over space (for the optimal predictor set) are displayed in  
338 Figure 7. Plot A shows the forecast of spatial hospitalization based on geospatial tweet  
339 positivity and city scale hospitalization. Predicted hospitalization based on Tweet positivity  
340 suggested there would be high hospitalization pressure  $H_P$  (Eq. 5.8) in areas, such as Narella,  
341 Gurugram and Dwarka (SW part of the city), which were unaccounted for by the monitoring  
342 system just focused on bed occupancy (and yet on models based on that occupancy shown  
343 in plot C and D). The highest peak of  $H_P$  is 160 and the average of healthcare pressure  
344 over space is very close to the average of hospitalization at the city scale. However, the  
345 geographical distribution of healthcare pressure is different from the distribution of hospi-  
346 tals because geokriging is extending spatially the positivity-hospitalization relationship (that  
347 shows an inverse proportionality between these variables) that is beyond hospital locations.  
348 Nonetheless, tweet locations highly predict hospital locations as binary variables (Fig. 7B).

349 When performing interpolation via geokriging based on hospital-scale data alone (Fig.  
350 7D), high hospitalization was predicted in the center of the city, with gradients of hospital-  
351 ization decreasing outwards. This predicted hospitalization reflects ( $\sim 80\%$ ) the distribution  
352 of bed occupancy as expected. The predicted hospitalization considering hospital-scale occu-  
353 pancy and positivity (Fig. 7C) matches 85% the hospitalization based on hospital data only  
354 (Fig. 7D). The former is however predicting higher hospitalization in other areas beyond  
355 hospital areas, and this emphasizes the fact that the model is also predicting healthcare pres-  
356 sure as individuals likely in need of hospitalization. Note that the range of hospitalization for  
357 predictions of plots C and D in Fig. 7 are the same with maximum cumulative hospitalization  
358 equal to  $\sim 65$  for the period 21 July-11 August 2020.

359 Figure 8 shows the calibration and validation of the ARIMA model which is useful for  
360 selecting the optimal set of predictors. The results of ARIMA forecasts with different models  
361 in terms of predictors are shown for cases, cumulative and new hospitalizations for New  
362 Delhi. ACF is ARIMA based on epidemiological data only, while all other ARIMA models  
363 are based on positivity, Tweet volume, Tweet volume and positivity combined. The model  
364 that minimizes the mean absolute percentage error (MAPE, in insets) is based on positivity  
365 only because of its highest predictive power for fluctuations in healthcare pressure (cases and

hospitalization). However, the model with volume and positivity has similar MAPE because of the ability of volume to predict the largest extreme variations in hospitalization. MAPE is larger for new hospitalization than cumulative hospitalizations due to the larger stochasticity of the former than the latter over time. The departure of forecasted values from observations is the gap index in the dashboard (Fig. 5).

The  $(p, d, q)$  parameters of the ARIMA model (Section 5.4.1) manifesting seasonality, memory and fluctuations are on average  $[0, 1, 1]$  for all models including ACF,  $[0, 1, 2]$  toward the end of the monitored period that highlights the increase importance of fluctuations, and  $[1, 1, 2]$  for volume and positivity that highlights the higher seasonality of tweet volume and ability to capture larger extremes.  $(p, d, q)$  parameters increase if misinformation is used when predicting hospitalization and cases, and this is in synchrony with our findings that non-linear predictability increases because of the higher memory long-range effects of misinformation. Average results of social and epidemiological variables for New Delhi are in Table 1 considering different areas of the city and time periods.

### 3 Discussion

We have demonstrated the use of InTo to calculate tweet positivity to forecast and predict the spatio-temporal spread of COVID-19 healthcare pressure. However, the model can be applied to any disease or public health phenomena of interest via properly tuning the forecasting models. In New Delhi we inferred that the population was relatively positive in the messaging, expressing mostly trust, despite the high case load and hospitalization. This weak negative correlation manifesting risk aversion – due to the expected decrease in positivity for increases in hospitalization – was statistically useful for predictability purposes considering both geostatistical kriging and ARIMA models that use correlation values (Eq. 5.3. and 5.7).

We showed that hospitalizations could be expected to concentrate in certain areas of the city, suggesting those clusters to be the focus of additional public health surveillance and healthcare resources since new hospitalizations may occur. We found that misinformation does affect the accuracy of the model and provides another illustration of the impact of misinformation: it can impact even our ability to properly forecast healthcare pressure but not necessarily negatively (in terms of reduction of prediction accuracy) throughout the pandemic. This impact was found to be positive, yet improving prediction accuracy, at the beginning of the epidemic (despite the higher volume of misinformation) and negative at the end of the epidemic likely because the delayed effect of misinformation spreading.

### 3.1 Data Uncertainty

The success of any intelligence tools rests also on the availability of data. Better quality data can likely support more accurate and more meaningful forecasts. Better data refers not only to the representativeness of the data but also to the granularity and compatibility of the data as well in relation to what is predicted. In terms of granularity, this could be hospital level rather than state or national level hospitalization data for example. We showed in Fig. 7 that the geostatistical kriging model performs much better – in terms of predicted hospitalization – when spatially explicit hospital data are provided, particularly when the objective is also to capture reported bed occupancy rather than average expected hospitalization at the city scale solely. Compatibility would mean not only using universally accepted terminology, but formatting the data in the same way to ease data processing. Certainly a huge discrepancy exist between social and epidemiological data (considering spatial and temporal resolutions as well as data volume), and then data processing becomes a time consuming process potentially carrying systematic uncertainties. Technology exists to translate data which is formatted differently, but it remains important that data stewards communicate with epidemiologists, “infodemiologists” and decision makers to determine a usable design. This is particularly important in the context of pandemics and emerging infectious diseases although localized.

Our concern is directed more towards epidemiological data rather than social media data. Social media users generate terabytes of data and many platforms have policies that allow restricted access to data, especially for academic purposes or some other public good purpose. However, epidemiological data has proven to be more difficult to collect and share. This would take effective coordination as hospital managers and public health officials collate and share data via application programming interfaces (API) for highest efficiency and timeliness in generating results.

### 3.2 Population Representativeness of Data

An issue connected with data availability is the matter of representation, that is, the extent to which the data include enough heterogeneity to reflect the complexity of the population for which the data set is assembled. This is particularly relevant to social media data such as Twitter data. The demographics of users can differ significantly by biology, socio-cultural and economic class, location and the availability of technological infrastructure (Silver et al., 2019; Sadah et al., 2015; Vashistha et al., 2015; Duggan and Brenner, 2013) so individual/community experiences and perspectives can differ from the wider population (Mellon

and Prosser, 2017). Even the choice of language might limit the representativeness of data used in the model: InTo currently uses English, which is spoken in India, but not by a majority. One also has to consider the inclusivity of the search term. Our use of 'OR' instead of 'AND' made our search more inclusive rather than restrictive thereby increasing the potential volume of tweets returned. Other choices would have certainly provided other predictability indices; and then one of the future improvements would be extracting the set of constraining hashtags that maximize predictions overall among all possible choices of hashtags. However, this choice would require a much higher computational cost and, in addition, fitting data the closest (versus providing the full range of feasible predictions in a Maximum Entropy perspective) is not always the optimal choice due to the presence of systematic uncertainty in data. Therefore, our current InTo version is not necessarily bounding the model-data gap considering all feasible factors (from language to hashtags), nor a fully causal investigation, but a model defining the simplest and most informative inputs and outputs to represent dynamics of population patterns. Further work will define more clearly importance of underlying factors and the absolutely optimal model form.

Tweets in a city contain information of spatially separated events about the same process; thus spatial spread of COVID and top tweeted pairs can be calculated over geolocated Tweets. Posting time and content (related to volume and positivity) is very weakly dependent on the social media platform. Additionally, social media users tend to interact outside of their usual social networks or real-world socio-economic class much more on these platforms (Silver et al., 2019), creating opportunities for groups absent from these platforms to be heard in a latent way. Furthermore, tweets report information that may not be reported by official media and/or that may circulate in real life events (e.g. just spoken information). This is also the reason for which InTo can be used by users as a reporting information/misinformation tool via registering their Twitter account. We suggest this “Digital Health” feature particularly relevant for healthcare workers.

Twitter penetration can differ between and within countries, but tweets still show high relevance for predicting spatio-temporal patterns of infections and hospitalization. Additionally, emotional affects are highly linked to local non-Twitter media and languages, as we see high volumetric correlation with local newspapers articles and retweets of English tweets in local languages. Certainly, demographic and other features of the tweeting population are relevant for how the virus spread but not the whole complexity is needed for forecasting purposes in the short and long term. Nonetheless, this version of InTo is a proof of concept version and will likely investigate and include other social media platforms, languages,



information features, visualization options, diseases and socio-environmental phenomena in future versions for investigating processes and practical applications.

### 3.3 Predictive Causality and Forecasting

Even when considering the issues of data availability and representativeness, the advantage of InTo is that it focuses on patterns rather than causation. InTo does not purport to have found nor to be exploiting a causal relationship between tweet positivity and healthcare pressure. Rather, it exploits spatio-temporal patterns and correlations that might not be physically significant (although arguable in an information dynamic sense), but that are nonetheless practically useful probabilistically. The relationship between sentiments and behaviors are quite complex, and there are many other variables in the complex reality of phenomena considered that are however not all needed when forecasting population outcomes. There are population factors such as sex, socio-economic status, proximity to affordable healthcare facilities and the availability of insurance or some other means of paying that certainly impact real processes of individuals. There may even be socio-political realities at play that force individual behavior. However, the key goal of InTo – in a complex system science purview – is the prediction of population patterns considering the most essential predictors without making any assumption on the underlying processes. Complicating the model comes at a cost, not just in the acquisition of data – because such data may not be available or costly to acquire – but also in the applicability of the resultant model that would be highly sensitive, extremely hard to calibrate and full of unchartable uncertainties. A model that enables reliable forecasts with a reasonable level of accuracy given a variety of scenarios should be the ultimate aim of any information system model.

In InTo a forecast refers to the estimation of future outcomes (in short term) which uses data from previous outcomes, combined with recent or future trends. Forecasts like those from the application of ARIMA models imply time series and future point estimates, while predictions do not. A prediction is based on probabilistic patterns (e.g. probability distributions, trends, and total uncertainty reductions) and yet of “possible outcomes” in the long-term. This is the case of geokriging and the pattern that can be obtained by using the predictability indicator (Eq. 5.12). Forecasting does not imply predictability nor the contrary, but in principle, optimized forecasting implies strong predictability for the whole time period considered. Vice versa, predictability of patterns does not guarantee the ability to have highly accurate time point estimates. InTo is providing both in order to support public health in almost real-time decision making and long term sensitivity of social surveillance for

497 epidemiological outcomes.

### 498 3.4 Value of Misinformation

499 Identifying misinformation is a chief concern in infodemiology via infoveillance, not to mention  
500 in other areas of society like sociology and politics. Methods that use the probabilistic and  
501 lexical features of text in order to determine whether they represent misinformation (Li et al.,  
502 2019) abound. These methods depend on datasets that contain messages which have already  
503 been labelled misinformation by experts a priori. The set of misinforming messages considered  
504 by inTo includes tweets already directly labelled as or questioned to be misinformation by  
505 users, having most likely already gone through a vetting process. The advantage of this  
506 approach is the use of a human- and crowd-based classification which overcomes the challenges  
507 of assumption-driven lexical analysis by model. Interestingly, a posteriori we confirmed (via  
508 reviewing Tweets one by one and considering their incorrect or false information) that the vast  
509 majority ( $\sim 95\%$ ) of misinformative tweets are truly misinformation and this misinformation  
510 set showed much larger dissimilarity – in terms of word diversity, volume divergence and  
511 asynchronicity – with respect to cases and hospitalization than the full tweet set. This  
512 emphasizes how dynamical properties of information are essential in categorizing different  
513 types of information, as well as how crowd-based self-reporting is relevant. In the literature  
514 there are still some debates about this topic but those seem platform dependent. For example,  
515 Jiang and Wilson (2018) suggested that user comments do not provide sufficient predictive  
516 power when attempting to classify misinformation, but a recent study (see Serrano et al.  
517 (2020)) successfully utilized user comments on YouTube videos instead of parsing these videos  
518 to classify misinformation with high accuracy.

519 Our results found that misinformation-related tweets provided at times more time-point  
520 accurate forecasts of healthcare pressure than forecasts based on all tweets. We observe  
521 that misinformation positivity shifts the forecast error based on all tweets to higher positive  
522 values (implying positive VoMi); yet, misinformation is slightly contributing to overprediction  
523 but considering its magnitude this overprediction is positive in consideration of surveillance  
524 underreporting and other systematic errors. This is not to say that misinformation is good  
525 in an absolute sense; in fact, it remains important that accurate facts are disseminated to  
526 people as the consequence of acting on incorrect information could imply wrong behavior  
527 leading to higher cases and hospitalization. Rather these findings show that misinformation  
528 – in its positivity rather than volume or messages – is useful for forecasting. This is related  
529 to the use of positivity as a novel aspect in characterizing social media content and to the

fact that positivity fluctuations of quickly generated misinformation tend to have long-term consequences on the predictability of the unfolding epidemic (misinformation that of course can have impact on the social behavior of populations). This is manifested for instance by a higher predictability indicator of misinformation (Fig. 5) as well as the higher  $(p, d, q)$  parameters of the ARIMA model (Section 5.4.1). Additionally, the full tweet information may contain too much “entropy” of messages that do not quite reflect people sentiments about the epidemic despite not being misinformation. Thus, public health organization could use positivity embedded in misinformation to protect the public, and then seek to eradicate.

### 3.5 Social Value of InTo

The most immediate value to society of InTo is through appropriate social media signal monitoring and by complementing traditional epidemiological surveillance which allows optimal healthcare planning during public health crises. As a novel and innovative infoveillance cyberinfrastructure (because available online and systematized in its function), apart from monitoring the spread of social chatter, InTo enables the public health system to properly plan for inevitable fluxes of people in need of care.

Public health officials and healthcare institutions need a way to cost-effectively determine whether they are able to meet the impending healthcare demands via considering both information and disease epidemics that we showed to be non-trivially and strongly coupled. Additionally, InTo enables public health officials to evaluate customer satisfaction of the healthcare system during the epidemic/pandemic. This is performed by evaluating sentiments of words related to healthcare in terms of emotions, positivity and specific content of social chatter. Content that can point out specific hospitals, physicians and treatments, as well as users. Thus, individuals are able to review what the general public posts as problems on social media about the local healthcare infrastructure and global issues. Also, information about which institutions are operating beyond their capacity, and what particular department may be operating poorly or successfully is available. Yet, InTo responds the need of predictive, personalized and precise health in an unprecedented way by both capturing information-driven salient population patterns and individual needs.

By monitoring public expressions, InTo provides some insights into emotional affects of the population in response to disease spread. This can also illuminate the importance of psychological states in response to these crises, which may be precursors to post traumatic stress disorders (PTSD). Other studies (Mowery et al., 2017; Wilson et al., 2014a) showed

562 how word choices reflect mental health states in long term and these may be predicted by  
 563 performing a systemic functional network analysis of the tweet text extracted by InTo. This  
 564 would also further link latent social and epidemiological outcomes explicitly.

565 Finally, InTo enables to monitor the spread of misinformation during public health and  
 566 social crises, as well as evaluate the impact of any intervention, in the form of risk communi-  
 567 cation, they enact. InTo provides volumetric measures of misinformation generation on social  
 568 media over time and geographical domain, as well as quantifies how misinformation affects  
 569 forecasts of case and hospitalization (i.e. VoMI) that potentially relate to real-world misbe-  
 570 havior dependent on circulating misinformation. Therefore, the performance of interventions  
 571 against misinformation can be measured by the volume of misinformation that is reduced  
 572 as well as by the uncertainty reduction in forecasts. In this sense, InTo provides an extra  
 573 evaluation of the surveillance system by considering misinformation as extra uncertainty or  
 574 uncertainty reduction, depending on its negative or positive impact, on prediction accuracy.  
 575 Comparison of multiple information sources and model predictions across multiple criteria  
 576 over time, is a rigorous and efficient way to evaluate surveillance systems and likely  
 577 detect the most reliable source of data (Vilas et al., 2017).

578

## 579 4 Conclusions

580 Infodemic Tomography (InTo) is proposed as a cybertechnology to monitor and visualize  
 581 the spatio-temporal co-causal variability of social media positivity and healthcare pressure  
 582 (as cases, hospitalization and misinformation separately) during epidemics and public health  
 583 crises. The most salient points to mention about InTo are listed below.

- 584 • A clear linkage between epidemiological and information dynamics (in terms of posi-  
 585 tivity) is detected via linear and non-linear patterns that are potentially revealing risk  
 586 perception or information availability in populations. These patterns are useful for pre-  
 587 dictions of epidemic dynamics, complementing traditional surveillance, and analyses  
 588 of social media dynamics (generation, absorption, spreading, diversity and positivity)  
 589 that have the potential to design risk communication strategies which aim to enhance  
 590 or correct information shared in the target populations.
- 591 • Location of tweets is deemed relevant to predict hospitalization where it is officially re-  
 592 ported (interestingly, ~60% of predictions of hospitalizations coincide with the reported

total bed occupancy in the test city of New Delhi and in locations where people are potentially in need of hospitalization. Yet, geospatial tweets (and associated positivity) are convenient transfer functions of epidemiological information to small space-time scales and inform about potential fluxes of healthcare demand that are useful for dynamic healthcare management. Forecasts of cases and hospitalization are provided at very high resolution ( $\sim m^2$ ) one week in advance by using a linearized ARIMA model. Risk and gap indicators are provided to measure the trend and model-gap difference of the epidemic weekly. A predictability indicator (normalized transfer entropy) is developed to monitor the uncertainty reduction of Twitter positivity for epidemiological dynamics, thus to test the predictive causality versus the forecasting of the ARIMA model.

- Misinformation is extracted by directly mining population-reported misinformation (via misinformation-related hashtags) and can be tested a posteriori via manual classification with public health officers cooperation and automated model-driven testing of dissimilarity (divergence, asynchronicity and diversity) from the systemic COVID-19 information over time. The Value of Misinformation (VoMi) is introduced as the impact on forecast accuracy calculated as the difference of gap indices (potentially negative over time) for the systemic and misinformation datasets. VoMi trends are city-specific and negative if they are increasing over time because they imply high impact of misinformation on short-term forecasting. VoMi is typically low or negative because it is highly non-linear and yet, not very informative of forecasting sudden events, but it carries higher predictability (as uncertainty reduction) for delayed long-term extremes and probabilistic patterns.

InTo encapsulates the future of public health management with the the fusion of multiple surveillance streams: from traditional epidemiological and healthcare data to model-inferred social sentiment data. As technology develops and the public creates and consumes information via internet, epidemiology will need to consider the spread of social information not only as a problematic element but as a solution for disease tracking and optimal risk communication. For instance, ad-hoc social messages by authorities can counteract misinformation that is sensed online, as well as social media inferred cases (or model predicted) can complement traditional public health surveillance. InTo shows that sentiments from digital messages can forecast the incidence and spread of healthcare pressure for areas besieged by a public health crisis. In terms of forecast, it is near-real time, accurate, reasonably inexpensive and easy to use in a computational sense. Infoveillance tools like InTo can only get better with higher

627 quality data from traditional surveillance systems on which validation should be performed,  
628 but more importantly with the collaboration between developers and stakeholders to effec-  
629 tively create solutions that are useful for effective decision and policy making. Future work  
630 will potentially entail expanding social media platforms and diseases to be monitored. Other  
631 validation experiments to improve InTo accuracy and utility are needed in data-rich areas.  
632 Via collaborations with public health officers, stakeholders and volunteers with interests in  
633 social computing we will seek for releasing InTo as a globally implemented cyberinfrastructure  
634 for public health research and practice.

## 635 5 Material, Methods and Implementation

### 636 5.1 Twitter Data Mining and Preprocessing

637 Data collection occurred weekly beginning in April 2020. Only English language tweets  
638 within a geographical bounding box (reflecting the target geographical area of the cities) were  
639 retrieved from Twitter using the `rtweet` package (Kearney, 2019). The choice of English was  
640 dictated by the lack of robust computational tools usable for other language translations  
641 (also considering the big-data size of tweets) and the complexity of the languages for the  
642 country considered (i.e., Hindi, Marathi, Thai, and Indonesian); the latter would make the  
643 uncertainty in positivity scoring of words very high.

644 Search terms are hashtags that were identified given their rank on a list of the most pop-  
645 ular Twitter terms on a daily and weekly scale (the search was done by comparing <https://getdaytrends.com/> and <https://trends24.in/>). Our search query for the COVID *sys-*  
646 *temic information* was constrained to the hashtags “covid OR coronavirus OR quarantine OR  
647 stay home OR hospital OR covid OR covid19 OR covid-19 OR coronavirus OR quarantine  
648 OR stayhome OR hospital”. Thus, we downloaded close to 30,000 tweets daily between April  
649 15 and July 30, 2020 for New Delhi (defined as “National Capital Territory of Delhi” by Twit-  
650 ter in the box  $28^{\circ}41'25.9''N, 76^{\circ}83'80.7''E$  to  $28^{\circ}88'13.4''N, 77^{\circ}34'84.6''E$ ). We identified the  
651 *misinformation* dataset by extracting a subset of our downloaded tweets that contained the  
652 terms “misinformation”, “false”, “fake” or “lie”, directly reported by people in their tweets.  
653 These were tweets in which a user either identified information or other messages as mis-  
654 information or questioned whether that message or information was misinformation. We  
655 also identified tweets related to *healthcare* information by extracting those tweets contain-  
656 ing the key terms “hospital” or “test”. To preprocess these data we removed punctuation  
657 marks and uniform resource locators (urls) using the `tidytext` package (Silge and Robin-  
658 son, 2016), and we replaced abbreviations, symbols, contractions, ordinals and numbers with  
659 the words they represent using the `qdap` package (Rinker, 2020). `tidytext` was also used  
660 to unnest the unigrams (single words) and bigrams (sequential word pairs) from each tweet.  
661 Lastly, word stemming was conducted using the `wordStem` function of the `SnowballC` package  
662 (<https://cran.r-project.org/web/packages/SnowballC/SnowballC.pdf>) for being able  
663 to score affine words in terms of positivity rather than disregarding these words.  
664

## 5.2 Epidemiological Data Mining and Preprocessing

At the time of our study, epidemiological data was not available for New Delhi specifically (i.e. the case study shown in this paper) nor for local hospitals within the analyzed domain, but rather for the state of Delhi, i.e. the National Capital Region (NCR). The dataset (kp, 2020) contained both crowd-sourced and official data from the Ministry of Health and Family Welfare. It included the number of cases and cured, discharged or migrated individuals in the state since March 15, 2020 when India registered its first case. For these motivations we calculated the new daily cases  $\Delta I = I(t) - I(t - 1)$  where  $I$  stands for cases, and new hospitalization as  $\Delta H = H(t) - H(t - 1)$  where hospitalization  $H(t) = I(t) - R(t)$  are cases minus the number of patients cured, discharged or migrated. Later we located hospital level data from information reported by the New Delhi from the Ministry of Health and Family Welfare (<https://coronabeds.jantasamvad.org>) which indicated the daily number of hospital beds occupied within a geo-located area. The vast majority of these hospitals resulted to be private hospitals. We conducted validation of our spatio-temporal forecasting model by comparing city-scale calculated hospitalization versus hospital-scale data for the same city. As for Mumbai, the situation was analogous to New Delhi; data of cases and hospitalization was only available at the state scale, i.e. Maharashtra. Thus, cases and hospitalization of Mumbai was calculated as  $\sim 50\%$  of the whole state as evidence supported. For Bangkok the same calculation was performed where original data are from <https://www.worldometers.info/coronavirus/country/thailand/>. Cases are 50% of national cases and hospitalization are 50% of active cases that are used by Thailand as the measure for hospitalization. Active cases in Thailand are defined as total cases minus total deaths and recovered patients, and “represents an important metric for Public Health and Emergency response authorities when assessing hospitalization needs versus capacity” (quoted by the Thailand Ministry of Health). Jakarta was the only city in our InTo application that provided city scale data of cases and hospitalization as independent variables. Data for Jakarta is from the Jakarta Health Department data reported to the Ministry of Health of Indonesia and displayed in <https://corona.jakarta.go.id/en/data-pemantauan>. For daily cases, data displayed in the time series labeled National Jakarta Trend are used. For hospitalization, data displayed in the time series “PDP Data Accumulation Table and Cases Data Accumulation Table” are used. We considered the sum of the reported number of patients currently in hospitals (PDP Data Accumulation Table) and the reported number of patients in intensive care (Cases Data Accumulation Table) as the cumulative hospitalization.



### 698 5.3 Sentiment Quantification

699 Sentiment analyses performed for InTo involved quantifying both categorical emotions and  
700 positivity of each text corpus given unigrams (words) within extracted tweets. The `labMT`  
701 lexicon (Dodds et al., 2011), accessed via the `qdap` package, was used to measure the positivity  
702 and the `nrc` lexicon (Mohammad and Turney, 2010), accessed via the `tidytext` package, was  
703 used to evaluate emotional affects (or categories) in a tweet. The continuous (real number)  
704 positivity of a tweet ( $P$ ) was quantified as:

$$P = \sum_{i=1}^N p_{avg}(w_i) \cdot \frac{f_i}{\sum_{j=1}^N f_j} \quad (5.1)$$

705 where  $p_{avg}(w_i)$  is the positivity value of each word ( $w_i$ ) as indicated in the labMT lexicon,  
706 and  $f_i$  is the frequency of each word. The daily positivity ( $\bar{P}_t$ ), given  $N_t$  number of tweets  
707 on day  $t$  is calculated by

$$\bar{P}_t = \frac{\sum_{j=1}^{N_t} P_j}{N_t} \quad (5.2)$$

708 where  $j$  is indicating all tweets in the day considered. The emotion of a tweet was con-  
709 sidered to be the distribution of the affect categories (for example, anger, surprise, joy, etc.)  
710 associated with each word of a tweet. We noted the affect categories associated with each  
711 unigram and then counted the number of times each affect category appeared in a tweet and  
712 in a day. Weekly calculations of positivity and emotion categories are calculated considering  
713 average value of sentiments at the weekly scale.

714

## 715 5.4 Forecasting

### 716 5.4.1 ARIMA temporal forecasting

717 InTo perform weekly temporal forecasts of new cases and hospitalizations as a function of  
718 tweet positivity and historical epidemiological events. A two-step non-seasonal ARIMA( $p, d, q$ )  
719 model is used for temporal forecasting where parameters  $p$ ,  $d$ , and  $q$  are non-negative integers;  
720  $p$  is the order (number of time lags) of the autoregressive model considering long term trends  
721 (e.g. seasonality),  $d$  is the degree of differencing (the number of times data are subtracted to  
722 past values) that considers memory for non-seasonal events, and  $q$  is the order of the moving-

average model for errors establishing their temporal impact. Because  $(p, d, q)$  parameters and coefficients are updated weekly in order to optimize forecasts, the model can be considered non-linear despite its linear formulation. Temporal forecasts were calculated using a non-seasonal ARIMA model as implemented in the **fable** package (O'Hara-Wild et al., 2020). The two-step forecast is done because first positivity is forecasted for the week following the one considered and after cases and hospitalization are forecasted based on future positivity. The analytic form of the ARIMA model is written for  $y = \Delta H$  as new hospitalization that is the primary target of InTo; however,  $y$  can generally be positivity or cases based on the selected predictand. Thus, hospitalization is forecasted as:

$$\Delta H_t^d = \beta_0 + \beta_1 \bar{P}_t + \phi_1 \Delta H_{t-1}^d + \cdots + \phi_p \Delta H_{t-p}^d + \theta_1 \varepsilon_{t-1} + \cdots + \theta_q \varepsilon_{t-q} + \varepsilon_t \quad (5.3)$$

where  $\Delta H$  is differenced to an order of  $d$  (not that  $d$  is an index and not a power exponent),  $\beta_0$  is a constant,  $\beta_1$  is the regression coefficient for average positivity  $\bar{P}_t$ ,  $\phi_1 y_{t-1}^d + \cdots + \phi_p y_{t-p}^d$  is an autoregressive model of order  $p$  and  $\theta_1 \varepsilon_{t-1} + \cdots + \theta_q \varepsilon_{t-q} + \varepsilon_t$  is a moving average model of order  $q$ . The error terms  $\varepsilon_t$  of  $\Delta H$  are assumed to be independent and identically distributed sampled from a normal distribution with zero mean. Thus,  $\varepsilon_t$  is a white noise factor.

Default settings of the ARIMA function in the **fable** package was selected as it automatically determines the values of  $p$ ,  $d$  and  $q$  that minimize the Akaike Information Criterion (AIC). We retrained our model weekly, using the entire history of positivity and epidemiological data to date. We utilize an ex-post forecasting approach where we first project the next week's values of positivity by applying the ARIMA model to tweet positivity. The ARIMA model is of a similar form to Eq. 5.3, except that positivity is the outcome value and the  $\beta_1 \bar{P}_t$  term is excluded. Following this we used the ARIMA model to forecast cases and hospitalizations considering the ARIMA linearized relationship between the history of epidemiological factors and tweet positivity and the projected values of positivity. Equivalently, without altering the ARIMA structural form in Eq. 5.3, we predicted new hospitalization considering different predictands, i.e. tweet volume, volume and positivity, or hospitalization only to select the optimal model with the highest prediction accuracy.

## 749 5.4.2 Geostatistical forecasting

750 We predicted the spatial spread of healthcare pressure with geostatistical kriging consider-  
 751 ing the inferred linear relationship between positivity and cumulative hospitalization at the  
 752 city scale. This relationship is linked to the  $\beta_1$  exponent in the ARIMA model of Eq. 5.3  
 753 and is updated every week. A similar modeling was performed in the past by Berke (2004).  
 754 Geostatistical kriging was performed using the `automap` package (Hiemstra et al., 2008).  
 755 We restricted data to the most recent two weeks of tweets and cumulative hospitalization  
 756 to ensure that there was enough geo-spatial tweet data salient to predict the last observed  
 757 hospitalization. This was also supported by the limited “memory” of positivity for hospi-  
 758 talization, reflected by low values of the ARIMA parameters  $p$  and  $d$ . As with the double  
 759 step prediction of ARIMA, first we extrapolate positivity over the whole geographical do-  
 760 main and after we perform a second geokriging to predict new hospitalization based on the  
 761 positivity-hospitalization relationship. Given the limited volume of geo-located tweets, we  
 762 used ordinary geo-statistical kriging because average is likely constant (Liang et al., 2018)  
 763 (as in our case) to interpolate positivity using the semi-variogram:

$$\gamma_P(\delta) = \frac{1}{2N(\delta)} \left\{ \sum_{i=1}^{N(\delta)} [P_{i+\delta} - P_i]^2 \right\} \quad (5.4)$$

764

$$\hat{P}_j = \sum_{i=1}^M \lambda_i(P_j) \cdot P_i \quad (5.5)$$

765 where  $\lambda_i(P_j)$  is a kriging weighting factor for the know value of the variable  $P$  at a sampled  
 766 location  $i$  and  $j \neq i$ . A function is a semivariogram only if it is a conditionally negative  
 767 definite function, i.e. for all weights  $\lambda_1, \dots, \lambda_M$  subject to  $\sum_{i=1}^M \lambda_i(P_j) = 0$  and locations  
 768  $i, \dots, M$  it holds:  $\sum_{i,j=1}^M \lambda_i \gamma_P(i, j) \lambda_j$ . This establishes the connection between predictions of  
 769 Eq. 5.5. and semivariogram of Eq. 5.4. The experimental semi-variogram of the data at the  
 770 observation location is fitted against a theoretical semi-variogram model of  $\hat{\gamma}_P(\delta_P)$ ; the latter  
 771 is an exponential, Gaussian or spherical semivariogram. One is thus making a distinction  
 772 between the experimental variogram that is a visualization of the observed possible spatio-  
 773 temporal correlation and the variogram model that is further used to define the weights of  
 774 the kriging function on which predictions are based.  $M$  is the number of (10,000) randomly  
 775 generated points which are interpolated using the kriging weighting factor  $\lambda_i(P_j)$  determined  
 776 by the semivariogram.

777 Next, we applied universal geostatistical kriging (Falah et al., 2017) to interpolate the

778 expected hospitalization  $\hat{H}$  over space considering the forecast based on the relationship  
 779 between twitter positivity and the state-level cumulative hospitalization. Universal kriging  
 780 is used because it assumes that the average is not constant as it is in our case. This is done  
 781 by using the following analytics:

$$\hat{\gamma}_H(\delta) = \frac{1}{2N(\delta)} \sum_{i=1}^{N(\delta)} [(\hat{H}_{i+\delta} - m) - (\hat{H}_i - m)]^2 \quad (5.6)$$

782

$$\hat{H}_j = m + \sum_{i=1}^M \lambda_i(H_j) \cdot (\hat{H}_i - m) \quad (5.7)$$

783 where  $\hat{\gamma}_H(\delta)$  is the predicted semivariogram of expected positivity based on  $m(\hat{P}) =$   
 784  $\sum_{l=0}^L \alpha_l f_l(\hat{P})$  that is a slow and continuous trend function (Kambhammettu et al., 2011)  
 785 capturing the linear relationship between hospitalization and tweet positivity among points  
 786  $l$ ; these points may be different from the whole set of points  $M$  over which interpolation is  
 787 performed. Finally, to determine the healthcare pressure  $H_P$  at each point  $i$  we used

$$H_{P_i} = \begin{cases} \hat{H}_i - \langle \hat{H}_T \rangle = \hat{H}_i - \frac{\sum_{i=1}^M \hat{H}_i}{M} & \text{if } > 0 \\ 0 & \text{otherwise} \end{cases} \quad (5.8)$$

788 where  $\langle \hat{H}_T \rangle$  is the expected average of hospitalization over the selected geographical do-  
 789 main, and  $M$  is the number of interpolated points. We applied the same model to spatially  
 790 explicit hospital bed occupancy in order to compare interpolations of hospitalization based  
 791 on state and hospital level data.

792

## 793 5.5 Predictability Indicators

794 Weekly indices are introduced to monitor the evolution of the pandemic, the short- and  
 795 long-term predictability of Twitter positivity and the departure between forecasts and ob-  
 796 servations. The *Risk Index* is set to measure the rate of change in epidemiological values,  
 797 yet in formulating indication of epidemic trends. The *Gap Index* is introduced as the differ-  
 798 ence between forecast predictions and observations normalized to previous observations. The  
 799 *Correlation Index* is calculated by estimating the Pearson correlation coefficient to quantify  
 800 the short-term forecast ability of positivity for epidemiological variables (new hospitaliza-  
 801 tions and new cases) via geokriging over space and via ARIMA over time. The first ARIMA

802 component and geokriging factors are linear functions of the linearized relationship between  
 803 positivity and epidemiological variables (Eqs. 5.3 and 5.7). To quantify the long-term pre-  
 804 dictability of highly diverging events, transfer entropy is introduced as the *Predictability Index*  
 805 that informs about the probabilistic predictability of positivity for epidemiological patterns  
 806 in terms of probability distribution functions rather than time point values. All indices are  
 807 analytically defined as:

$$R(Y_t) = (y_t - y_{t-1})/y_{t-1} = \Delta Y(\delta t)/100 \quad (5.9)$$

$$G(Y_t) = \hat{y}(t) - y(t)/y(t) = \Delta \hat{Y}_t/100 \quad (5.10)$$

$$\text{corr}(P, Y) = \frac{\sum_{t=1}^L (p_t - \bar{P})(y_t - \bar{Y})}{\sqrt{\sum_{t=1}^L (p_t - \bar{P})^2 \sum_{t=1}^L (y_t - \bar{Y})^2}} \quad (5.11)$$

$$TE_{P \rightarrow Y} = \sum p(Y_t, Y_{t-1}, P_{t-1}) \cdot \log \left( \frac{p(Y_t|Y_{t-1}, P_{t-1})}{p(Y_t|Y_{t-1})} \right) \quad (5.12)$$

808 where  $Y = I$  or  $\Delta H$  is indicating time series of cases or hospitalization, respectively,  
 809 and  $y$  indicates time point values.  $\bar{P} = \frac{1}{L} \sum_{t=1}^L p_t$  and  $\bar{Y} = \frac{1}{L} \sum_{t=1}^L y_t$ .  $L$  is the length of  
 810 time-series of  $P$  and  $Y$ .

811 The Value of Misinformation (*VoMi*) was defined as the difference of gap indices as:

$$VoMi(t) = G(Y_t)_S - G(Y_t)_M \quad (5.13)$$

812 where  $S$  and  $M$  stand for the systemic Twitter information and classified misinformation  
 813 set in predicting  $Y$  as cases or hospitalization. *VoMi* provides users with a measure of how  
 814 misinformation impact forecasts of epidemiological variables with respect to the systemic  
 815 tweet information considering both model and data uncertainty contained in the gap index.

816 Increasing values of *VoMi* (independently of the sign) indicate that the misinformation  
 817 tweet subset has increasing importance in forecasting versus the full tweet set. On average,  
 818 if *VoMi* is positive, misinformation does contribute non-negligibly to overpredict epidemio-  
 819 logical trends, whereas if it is negative it impacts positively and substantially the forecasts  
 820 proportionally to the magnitude of the misinformation gap  $G(Y_t)_M$ . This is evaluated for  
 821 the same model structure and epidemiological data uncertainty of the full tweet information.  
 822 It should be noted that both gap indices  $G(Y_t)_S$  and  $G(Y_t)_M$  can be negative and  $M \subseteq S$ ,  
 823 yet the relative (non-linear) balance between full information and misinformation (positivity)

824 predictability contribute to determining VoMi.

825 In a decision analytical sense VoMi is defined as the amount of resources a decision  
826 maker would be willing to pay for extra information that increase forecast accuracy be-  
827 fore an event occurs. The optimal information set  $\mathbf{I}_{opt}$  is defined as the one whose gap is  
828 minimized (assuming that data are perfect “error-free” information to match) and equal to  
829  $G(\mathbf{I}_{opt}) = G(\mathbf{I}_{sub}) - VoMi(\mathbf{I}_{opt}, \mathbf{I}_{sub})$  where  $VoMi = MI(P, H)$  that is the mutual informa-  
830 tion  $MI(P, Y) = \sum_p \sum_y p(p, y) \log \frac{p(p, y)}{p(p)p(y)}$  between positivity and cases or hospitalization.  
831 Mutual Information in an information-theoretic variable measuring the amount of information  
832 shared between two variables that is on average inversely proportional to the predictability  
833 indicator in Eq. 5.12 (i.e. the uncertainty reduction between variables).

## 834 5.6 Tweet Spread

835 For each week, we calculated and displayed the average daily tweet and retweet volume for all  
836 tweets and the misinformation related tweets. Time series of tweet and retweet volumes, as  
837 well as their corresponding average positivity, are displayed by InTo, which serve as indicators  
838 of spreading potential of COVID-19 related messages within and beyond the geographical  
839 domain considered. Additionally, the Twitter user of the most popular tweet in a week is  
840 shown when hovering over a point on the Tweet spread plot.

## 841 5.7 Dashboard Architecture

842 The InTo dashboard utilizes a client-server architecture designed and implemented using the  
843 **shiny** package (Chang et al., 2020) in R (R Core Team, 2020) that provides a convenient  
844 wrapper for interactive HTML widgets. This is similar to GLEaMviz architecture (Van den  
845 Broeck et al., 2011). The client component only allows users to visualize the results of InTo  
846 but many outputs, for example predictability indicators, are downloadable by users. All  
847 computations on the server are conducted in R using the established workflow (see Fig. 1).

## 848 InTo online

849 InTo online dashboards and data are at:

850 [https://nexuslab.shinyapps.io/InTo\\_Delhi/](https://nexuslab.shinyapps.io/InTo_Delhi/) for the city of New Delhi

851 [https://nexuslab.shinyapps.io/InTo\\_Mumbai/](https://nexuslab.shinyapps.io/InTo_Mumbai/) for the city of Mumbai

852 [https://nexuslab.shinyapps.io/InTo\\_Jakarta/](https://nexuslab.shinyapps.io/InTo_Jakarta/) for the city of Jakarta

853 [https://nexuslab.shinyapps.io/InTo\\_Bangkok/](https://nexuslab.shinyapps.io/InTo_Bangkok/) for the city of Bangkok

854

855 Into online manual, workflow, data sources and codes is at:

856 <https://rpubs.com/elroyg1/Into-walkthrough>

857

858 Into main code is at:

859 <https://github.com/elroyg1/InTo>

860

## 861 Data Ethical Approval

862 Twitter data are collected by leveraging Twitter’s free streaming API. A Twitter developer  
863 account was obtained as well as the necessary authentication tokens. The data set is avail-  
864 able in compliance with the Twitter’s Terms and Conditions ([https://developer.twitter.](https://developer.twitter.com/en/developer-terms/agreement-and-policy)  
865 [com/en/developer-terms/agreement-and-policy](https://developer.twitter.com/en/developer-terms/agreement-and-policy)), under which we are unable to publicly  
866 release the text of the collected tweets. Twitter developer account was obtained on May  
867 7, 2020. We are, therefore able to release Tweet IDs, which are unique identifiers tied to  
868 specific tweets. The Tweet IDs can be used by researchers to query Twitter’s API and obtain  
869 the complete tweet object, including tweet content (text, URLs, hashtags, etc) and authors’  
870 metadata. Our collection relies upon publicly available data (both epidemiological and Twit-  
871 ter data) and is hence registered as IRB (institutional review board) exempt by Hokkaido  
872 University.



## 873 **Author Contribution**

874 E.G. performed all calculations and data mining, developed the dashboard, and contributed  
875 to the writing.

876 J.L. supported the data mining and performed predictability index calculations.

877 M.C. conceptualized, analytically formalized, designed and guided the dashboard creation,  
878 and wrote the manuscript.

879

## 880 **Acknowledgements**

881 All authors acknowledge the collaboration and support from SEARO/WHO (project num-  
882 ber 2020/1015441-0). Victor del Rio-Vilas at WHO/SEARO is greatly acknowledged. E.G.  
883 acknowledges the Ministry of Education, Culture, Sports, Science and Technology (MEXT)  
884 for this PhD fellowship. M.C. acknowledges the funding from the FY2020 SOUSEI Support  
885 Program and Award for Young Researchers (awarded by the Executive Office for Research  
886 Strategy to the Top 20% scientists in terms of productivity and citations at Hokkaido Uni-  
887 versity) and the GI-CoRE GSB Station at Hokkaido University, Sapporo, Japan.

## References

- Susel Góngora Alonso, Isabel de la Torre Díez, and Begoña García Zapirain. Predictive, personalized, preventive and participatory (4p) medicine applied to telemedicine and ehealth in the literature. Journal of medical systems, 43(5):140, 2019.
- Joana M Barros, Jim Duggan, and Dietrich Rebholz-Schuhmann. The application of internet-based sources for public health surveillance (infoveillance): systematic review. Journal of Medical Internet Research, 22(3):e13680, 2020.
- Olaf Berke. Exploratory disease mapping: kriging the spatial risk function from regional count data. International Journal of Health Geographics, 3(1):18, 2004.
- Nicola Luigi Bragazzi. Infodemiology and infoveillance of multiple sclerosis in italy. Multiple sclerosis international, 2013, 2013.
- Winston Chang, Joe Cheng, JJ Allaire, Yihui Xie, and Jonathan McPherson. shiny: Web Application Framework for R, 2020. URL <https://CRAN.R-project.org/package=shiny>. R package version 1.4.0.2.
- Peter Sheridan Dodds, Kameron Decker Harris, Isabel M Kloumann, Catherine A Bliss, and Christopher M Danforth. Temporal patterns of happiness and information in a global social network: Hedonometrics and twitter. PloS one, 6(12):e26752, 2011.
- Maeve Duggan and Joanna Brenner. The demographics of social media users, 2012, volume 14. Pew Research Center’s Internet & American Life Project Washington, DC, 2013.
- Johannes C Eichstaedt, Hansen Andrew Schwartz, Margaret L Kern, Gregory Park, Darwin R Labarthe, Raina M Merchant, Sneha Jha, Megha Agrawal, Lukasz A Dziurzynski, Maarten Sap, et al. Psychological language on twitter predicts county-level heart disease mortality. Psychological science, 26(2):159–169, 2015.
- Gunther Eysenbach. Infodemiology and infoveillance: framework for an emerging set of public health informatics methods to analyze search, communication and publication behavior on the internet. Journal of medical Internet research, 11(1):e11, 2009.
- Annisa Nur Falah, Betty Subartini, and Budi Nurani Ruchjana. Application of universal kriging for prediction pollutant using gstat r. In IOP Conf. Series: Journal of Physics: Conf. Series, volume 893, pages 1–7, 2017.
- Riccardo Gallotti, Francesco Valle, Nicola Castaldo, Pierluigi Sacco, and Manlio De Domenico. Assessing the risks of” infodemics” in response to covid-19 epidemics. arXiv preprint arXiv:2004.03997, 2020.

920 Jeremy Ginsberg, Matthew H Mohebbi, Rajan S Patel, Lynnette Brammer, Mark S Smolin-  
921 ski, and Larry Brilliant. Detecting influenza epidemics using search engine query data.  
922 Nature, 457(7232):1012–1014, 2009.

923 Pari Delir Haghighi, Yong-Bin Kang, Rachelle Buchbinder, Frada Burstein, and Samuel Whit-  
924 tle. Investigating subjective experience and the influence of weather among individuals with  
925 fibromyalgia: a content analysis of twitter. JMIR public health and surveillance, 3(1):e4,  
926 2017.

927 P.H. Hiemstra, E.J. Pebesma, C.J.W. Twenhöfel, and G.B.M. Heuvelink. Real-  
928 time automatic interpolation of ambient gamma dose rates from the dutch ra-  
929 dioactivity monitoring network. Computers & Geosciences, 2008. DOI:  
930 <http://dx.doi.org/10.1016/j.cageo.2008.10.011>.

931 Md Saiful Islam, Tonmoy Sarkar, Sazzad Hossain Khan, Abu-Hena Mostofa Kamal, Sarkar  
932 Mohammad Murshid Hasan, Alamgir Kabir, Dalia Yeasmin, Mohammad Ariful Islam,  
933 Kamal Ibne Amin Chowdhury, Kazi Selim Anwar, Abrar Ahmad Chughtai, and Holly  
934 Seale. Covid-19?related infodemic and its impact on public health: A global social media  
935 analysis. The American Society of Tropical Medicine and Hygiene, 2020.

936 Shan Jiang and Christo Wilson. Linguistic signals under misinformation and fact-  
937 checking: Evidence from user comments on social media. Proceedings of the ACM on  
938 Human-Computer Interaction, 2(CSCW):1–23, 2018.

939 BVNP Kambhammettu, Praveena Allena, and James P King. Application and evaluation of  
940 universal kriging for optimal contouring of groundwater levels. Journal of Earth System  
941 Science, 120(3):413, 2011.

942 Michael W. Kearney. rtweet: Collecting and analyzing twitter data. Journal of Open Source  
943 Software, 4(42):1829, 2019. doi: 10.21105/joss.01829. URL [https://joss.theoj.org/](https://joss.theoj.org/papers/10.21105/joss.01829)  
944 [papers/10.21105/joss.01829](https://joss.theoj.org/papers/10.21105/joss.01829). R package version 0.7.0.

945 Devakumar kp. covid-19-india-data, 2020. URL [https://github.com/imdevskp/](https://github.com/imdevskp/covid-19-india-data)  
946 [covid-19-india-data](https://github.com/imdevskp/covid-19-india-data).

947 J Li and M Convertino. Taming network inference: Optimal information flow model. PNAS,  
948 2020. in review.

949 Quanzhi Li, Qiong Zhang, Luo Si, and Yingchi Liu. Rumor detection on social media:  
950 Datasets, methods and opportunities. arXiv preprint arXiv:1911.07199, 2019.

951 Ching-Ping Liang, Jui-Sheng Chen, Yi-Chi Chien, and Ching-Fang Chen. Spatial analysis of  
 952 the risk to human health from exposure to arsenic contaminated groundwater: A kriging  
 953 approach. Science of The Total Environment, 627:1048–1057, 2018.

954 Yang Liu, Brenda O Hoppe, and Matteo Convertino. Threshold evaluation of emergency risk  
 955 communication for health risks related to hazardous ambient temperature. Risk analysis,  
 956 38(10):2208–2221, 2018.

957 Savi Maharaj and Adam Kleczkowski. Controlling epidemic spread by social distancing: Do  
 958 it well or not at all. BMC Public Health, 12(1):679, 2012a.

959 Savi Maharaj and Adam Kleczkowski. Controlling epidemic spread by social distancing: Do  
 960 it well or not at all. BMC Public Health, 12(1):679, 2012b.

961 Craig J McGowan, Matthew Biggerstaff, Michael Johansson, Karyn M Apfeldorf, Michal  
 962 Ben-Nun, Logan Brooks, Matteo Convertino, Madhav Erraguntla, David C Farrow, John  
 963 Freeze, et al. Collaborative efforts to forecast seasonal influenza in the united states,  
 964 2015–2016. Scientific reports, 9(1):1–13, 2019.

965 Jonathan Mellon and Christopher Prosser. Twitter and facebook are not representative of  
 966 the general population: Political attitudes and demographics of british social media users.  
 967 Research & Politics, 4(3):2053168017720008, 2017.

968 Saif Mohammad and Peter Turney. Emotions evoked by common words and phrases: Using  
 969 mechanical turk to create an emotion lexicon. In Proceedings of the NAACL HLT 2010  
 970 workshop on computational approaches to analysis and generation of emotion in text, pages  
 971 26–34, 2010.

972 Danielle Mowery, Hilary Smith, Tyler Cheney, Greg Stoddard, Glen Coppersmith, Craig  
 973 Bryan, and Mike Conway. Understanding depressive symptoms and psychosocial stressors  
 974 on twitter: a corpus-based study. Journal of medical Internet research, 19(2):e48, 2017.

975 Mitchell O’Hara-Wild, Rob Hyndman, and Earo Wang. fable: Forecasting Models for Tidy  
 976 Time Series, 2020. URL <https://CRAN.R-project.org/package=fable>. R package ver-  
 977 sion 0.2.1.

978 A Ross Otto and Johannes C Eichstaedt. Real-world unexpected outcomes predict city-level  
 979 mood states and risk-taking behavior. PloS one, 13(11):e0206923, 2018.

980 Michael J Paul, Mark Dredze, and David Broniatowski. Twitter improves influenza forecast-  
 981 ing. PLoS currents, 6, 2014.

982 R Core Team. R: A Language and Environment for Statistical Computing. R Foundation  
983 for Statistical Computing, Vienna, Austria, 2020. URL <https://www.R-project.org/>.

984 M Radin and S Sciascia. Infodemiology of systemic lupus erythematosus using google trends.  
985 Lupus, 26(8):886–889, 2017.

986 Sudha Ram, Wenli Zhang, Max Williams, and Yolande Pengetnze. Predicting asthma-  
987 related emergency department visits using big data. IEEE journal of biomedical and health  
988 informatics, 19(4):1216–1223, 2015.

989 Tyler W. Rinker. qdap: Quantitative Discourse Analysis Package. Buffalo, New York, 2020.  
990 URL <http://github.com/trinker/qdap>. 2.3.6.

991 Marco Rocchetti, Gustavo Marfia, Paola Salomoni, Catia Prandi, Rocco Maurizio Zagari,  
992 Faustine Linda Gningaye Kengni, Franco Bazzoli, and Marco Montagnani. Attitudes of  
993 crohn’s disease patients: Infodemiology case study and sentiment analysis of facebook and  
994 twitter posts. JMIR public health and surveillance, 3(3):e51, 2017.

995 Shouq A Sadah, Moloud Shahbazi, Matthew T Wiley, and Vagelis Hristidis. A study of the  
996 demographics of web-based health-related social media users. Journal of medical Internet  
997 research, 17(8):e194, 2015.

998 Takeshi Sakaki, Makoto Okazaki, and Yutaka Matsuo. Earthquake shakes twitter users: real-  
999 time event detection by social sensors. In Proceedings of the 19th international conference  
1000 on World wide web, pages 851–860, 2010.

1001 Mauricio Santillana, André T Nguyen, Mark Dredze, Michael J Paul, Elaine O Nsoesie,  
1002 and John S Brownstein. Combining search, social media, and traditional data sources to  
1003 improve influenza surveillance. PLoS Comput Biol, 11(10), 2015.

1004 Juan Carlos Medina Serrano, Orestis Papakyriakopoulos, and Simon Hegelich. Nlp-based  
1005 feature extraction for the detection of covid-19 misinformation videos on youtube, 2020.

1006 Julia Silge and David Robinson. tidytext: Text mining and analysis using tidy data principles  
1007 in r. JOSS, 1(3), 2016. doi: 10.21105/joss.00037. URL [http://dx.doi.org/10.21105/](http://dx.doi.org/10.21105/joss.00037)  
1008 [joss.00037](http://dx.doi.org/10.21105/joss.00037).

1009 Laura Silver, Christine Huang, and Kyle Taylor. In emerging economies smart phone and  
1010 social media users have broader social networks. Pew Research Center, 2019.

1011 Linda Thunström, Stephen C Newbold, David Finnoff, Madison Ashworth, and Jason F  
1012 Shogren. The benefits and costs of using social distancing to flatten the curve for covid-19.  
1013 Journal of Benefit-Cost Analysis, pages 1–27, 2020.

- 1014 Carolina Oi Lam Ung. Community pharmacist in public health emergencies: quick to ac-  
 1015 tion against the coronavirus 2019-ncov outbreak. Research in Social and Administrative  
 1016 Pharmacy, 2020.
- 1017 Wouter Van den Broeck, Corrado Gioannini, Bruno Gonçalves, Marco Quaggiotto, Vittoria  
 1018 Colizza, and Alessandro Vespignani. The gleamviz computational tool, a publicly avail-  
 1019 able software to explore realistic epidemic spreading scenarios at the global scale. BMC  
 1020 infectious diseases, 11(1):1–14, 2011.
- 1021 Aditya Vashistha, Edward Cutrell, Nicola Dell, and Richard Anderson. Social media plat-  
 1022 forms for low-income blind people in india. In Proceedings of the 17th International ACM  
 1023 SIGACCESS Conference on Computers & Accessibility, pages 259–272, 2015.
- 1024 Victor Del Rio Vilas, M Kocaman, Howard Burkom, Richard Hopkins, John Berezowski, Ian  
 1025 Painter, Julia Gunn, G Montibeller, M Convertino, LC Streichert, et al. A value-driven  
 1026 framework for the evaluation of biosurveillance systems. Online Journal of Public Health  
 1027 Informatics, 9(1), 2017.
- 1028 WHO et al. 2019 novel coronavirus (2019-ncov): strategic preparedness and response plan,  
 1029 2020.
- 1030 Max L Wilson, Susan Ali, and Michel F Valstar. Finding information about mental health in  
 1031 microblogging platforms: a case study of depression. In Proceedings of the 5th Information  
 1032 Interaction in Context Symposium, pages 8–17, 2014a.
- 1033 Max L. Wilson, Susan Ali, and Michel F. Valstar. Finding information about mental health in  
 1034 microblogging platforms: A case study of depression. In Proceedings of the 5th Information  
 1035 Interaction in Context Symposium, IliX ?14, page 8?17, New York, NY, USA, 2014b. As-  
 1036 sociation for Computing Machinery. ISBN 9781450329767. doi: 10.1145/2637002.2637006.  
 1037 URL <https://doi.org/10.1145/2637002.2637006>.

## 1038 Table Captions

1039 **Table 1. Average Socio-epidemiological Values for New Delhi.** Average weekly val-  
1040 ues for hospitalization  $H$ , cases  $I$ , tweet volume, retweet and positivity ( $V$ ,  $R$ , and  $P$ ), as well  
1041 as Pearson correlation between positivity and hospitalization. Average  $VoMi$  also provided.  
1042 The Pearson correlation is proportional to the first regression coefficient of the ARIMA fore-  
1043 casting model and the geokriging factor of hospitalization predictions. The higher  $\text{corr}(P, H)$   
1044 the higher the potential risk aversion for the city (areas and time periods) considered. It is  
1045 empirically observed that the higher the risk aversion the lower the social (Twitter) genera-  
1046 tion of information and the healthcare pressure defined by combined case and hospitalization  
1047 magnitude.  $VoMi$  is expected to be higher for less risk-averting city areas (and time periods)  
1048 with higher incidence (thus misinformation is more predictive of cases and hospitalization)  
1049 and these areas/time periods should appear more local in terms of circulating information.

1050

## Figure Captions

**Figure 1. Conceptual and Computational Workflow of InTo.** The process begins with downloading both social media content and epidemiological data. Social media data is then disaggregated into content related to healthcare and misinformation, with the aggregated content retained for analysis as well. As for epidemiological data, the dashboard makes use of hospitalization and cases data for the disease considered. The next process is the extraction of features from social media content: for each subset, bi-grams, count information and sentiments are quantified. Metrics quantifying the relationships between sentiment and epidemiological data are then calculated. Once the linear regression coefficients are estimated, these are used to forecast the spatial and temporal variation of healthcare pressure, which is then visualized for users on the dashboard. To illustrate the process and output of InTo we examine the case of New Delhi, India.

**Figure 2. Dashboard Tab 1: Healthcare Pressure Spatial Predictions.** Users are presented with a heatmap, time series of tweet positivity, cases, new hospitalizations and cumulative hospitalizations. In addition, two text outputs inform the user about the predicted hospitalization and cases for the selected city and the difference between the current predicted values and the values predicted for last week. The heatmap visualizes the results of geokriging the spatial interpolation of hospitalization as a function of tweet positivity. Hotter areas are where patients potentially in need of hospitalization are concentrated.

**Figure 3. Spatial Forecasts.** Gradients of Healthcare Pressure, that is  $HP_i = \hat{H}_{T_i} - H_T$ , reflect potential movement of people in need of hospitalization (hospitalization fluxes). The sum of  $HP_i$  from geokriging over space is theoretically equal to the predicted cumulative hospitalization over time ( $H_T = \sum_t \Delta H(t)$ ) as a function of the new hospitalization (that are temporal hospitalization fluxes or healthcare pressure over time). An Effective Healthcare Pressure can be calculated as difference between normalized  $HP_i$  and healthcare capacity ( $HC_I$ ) as a function of area healthcare infrastructure resources (e.g. beds, ICUs, ventilators). Uncertainty in forecasts can also consider spatially explicit testing rate and surveillance capacity. In analogy to weather forecasts, gradient of pressure over space are the byproduct of gradient of pressure over time modulated by underlying environmental conditions.



**Figure 4. Dashboard Tab 2: Emotions, Top Bigrams and Tweets for Predictive Information, Misinformation and Healthcare.** In the Emotions and Misinformation section, users are shown two time series of emotional affect, a table of tweet texts with their retweet counts and positivity, and a visualization of the top bigrams for a selected week. The time series on the left presents the absolute volume of emotional affects while the time series on the right visualizes the proportional volume of each category. Users are given the opportunity to visualize the output for all tweets, or the subset of misinforming or healthcare tweets. They are also given the opportunity to select and send any tweet from the table to the administrators for inclusion in the misinformation subset of tweets. The administrators can redo the analysis of the impact and value of misinformation considering the newly identified misinforming tweets.

**Figure 5. Dashboard Tab 3: Predictability Indicators.** The Predictability section displays time series of risk, gap, predictability, and correlation indices along with the value of misinformation. In the left plots, users are shown these indices when the positivity of all tweets are used to forecast cases and hospitalizations. Middle plots show these indices when the positivity of the subset of misinforming tweets are used to forecast cases and hospitalizations. The right plots show time series of the value of misinformation (VoMi). For all plots, the x axis represents the time in weeks, while the y axis represents the value of the indicator as a percentage ratio. When users hover over a point, they are presented with the x-y coordinates.

**Figure 6. Dashboard Tab 3: Information Volume and Spreading Potential.** The Tweet Spread section visualizes the spreading potential considering all tweets and the spreading potential from the subset of misinforming tweets. The x axis represents time in weeks while the y axis indicates the tweet volume observed in that week. The dashed lines show the tweet volume for all tweets in that category while the solid line indicates the volume for the most retweeted tweets. The size of each point represents the mean retweet volume for that week, while the color represents the positivity of the most retweeted tweet observed the selected week. By hovering over a point the most retweeted tweet for that week is presented on the right.

**Figure 7. Spatial Validation of Geokriging Predictions of Cumulative Hospitalization.** Predicted and observed cumulative hospitalization ( $\hat{H}_T$  and  $H_T$ ) are calculated

1118 as a function of spatially explicit positivity  $P_i$  and hospital reported hospitalization (plot A  
 1119 and C) via geokriging. Plot A shows the prediction offered by the dashboard where spatial  
 1120 healthcare pressure  $HP_i = \hat{H}_{T_i} - H_T$  is determined as difference between local and total  
 1121 hospitalization at the city scale. Plot B and D report predictions of hospital location based  
 1122 on positivity and cumulative hospitalization based on reported bed occupancy only, respec-  
 1123 tively. The relationship on the top of each plot is reporting what is used in the geokriging  
 1124 calibration, while what is predicted is reported at the bottom. Squares indicate officially  
 1125 reported hospitals designated for COVID-19 patients, while blue points indicate geo-located  
 1126 Tweets. Predictions are for the period 21 July-11 August 2020.

1127

1128 **Figure 8. Hospitalization and Case Forecasting for Different Predictive Mod-**  
 1129 **els.** The results of ARIMA forecasts with different models in terms of predictors are shown  
 1130 for cases, cumulative and new hospitalization (top to bottom) for New Delhi. ACF is ARIMA  
 1131 based on epidemiological data only, while all other ARIMA models are based on positivity,  
 1132 Tweet volume, Tweet volume and positivity combined (red, blue, yellow, and green curves).  
 1133 Black dots are from observations at the city scale. All curves are at the daily resolution.

1134

City	$\bar{H}_t$	$\bar{I}_t$	$\bar{V}_t$	$\bar{R}_t$	$\bar{P}_t$	$\text{corr}(P, H)$	$VoMi$
New Delhi	100	1000	10,600	9	5.75	-0.5	0.00
Mumbai	500	1250	10,500	10	5.85	-0.1	0.10
Bangkok	1	4	1000	11	5.80	-2	-0.05
Jakarta	25	200	900	20	5.90	-1	-0.10

Table 1:

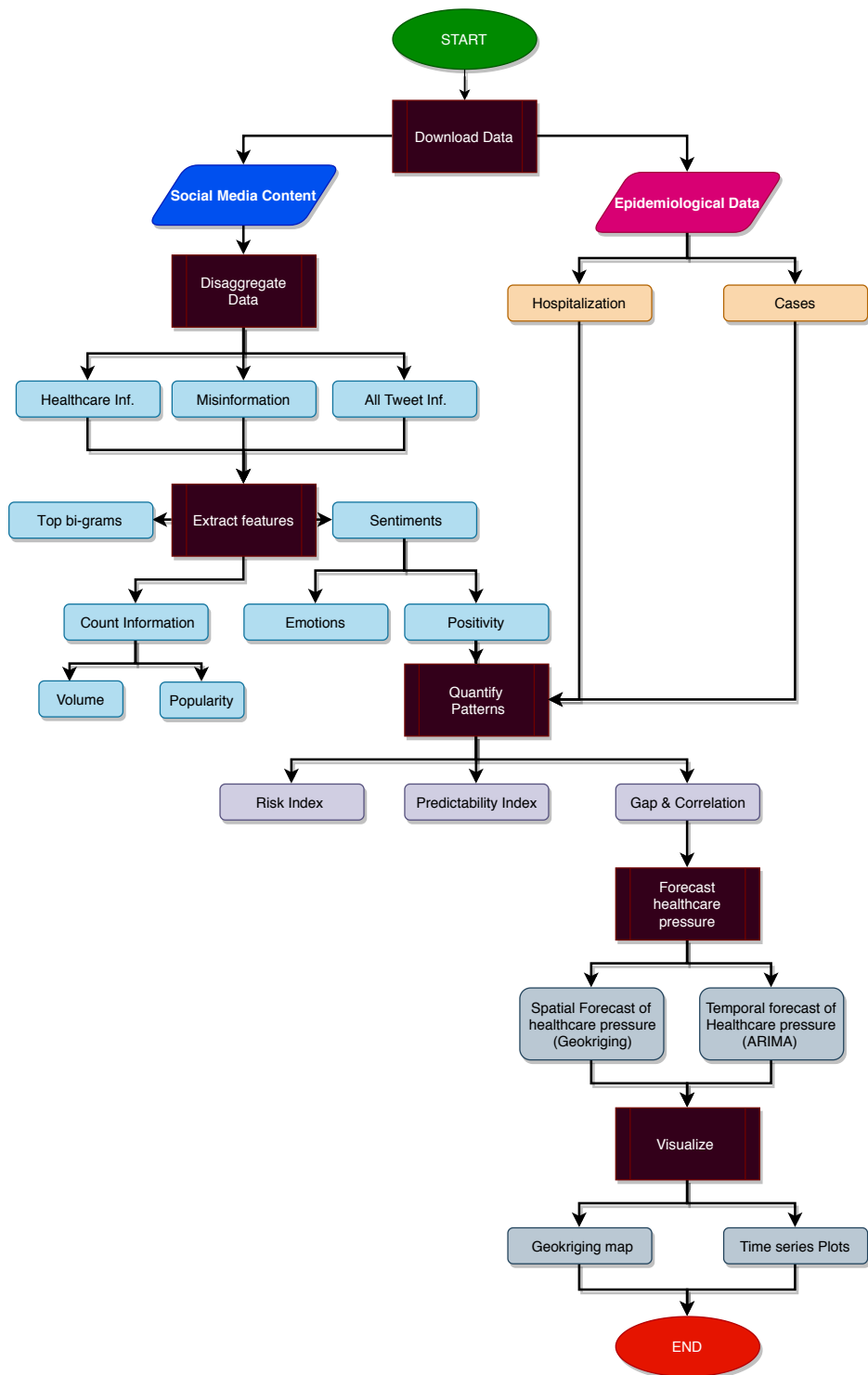


Figure 1:



The Infographic Tomogram for Delhi as at 2020-07-16

Predicted weekly hospitalization = -382  
Predicted weekly hospitalization change = 21

Predicted weekly cases = 1400  
Predicted weekly cases change = -143

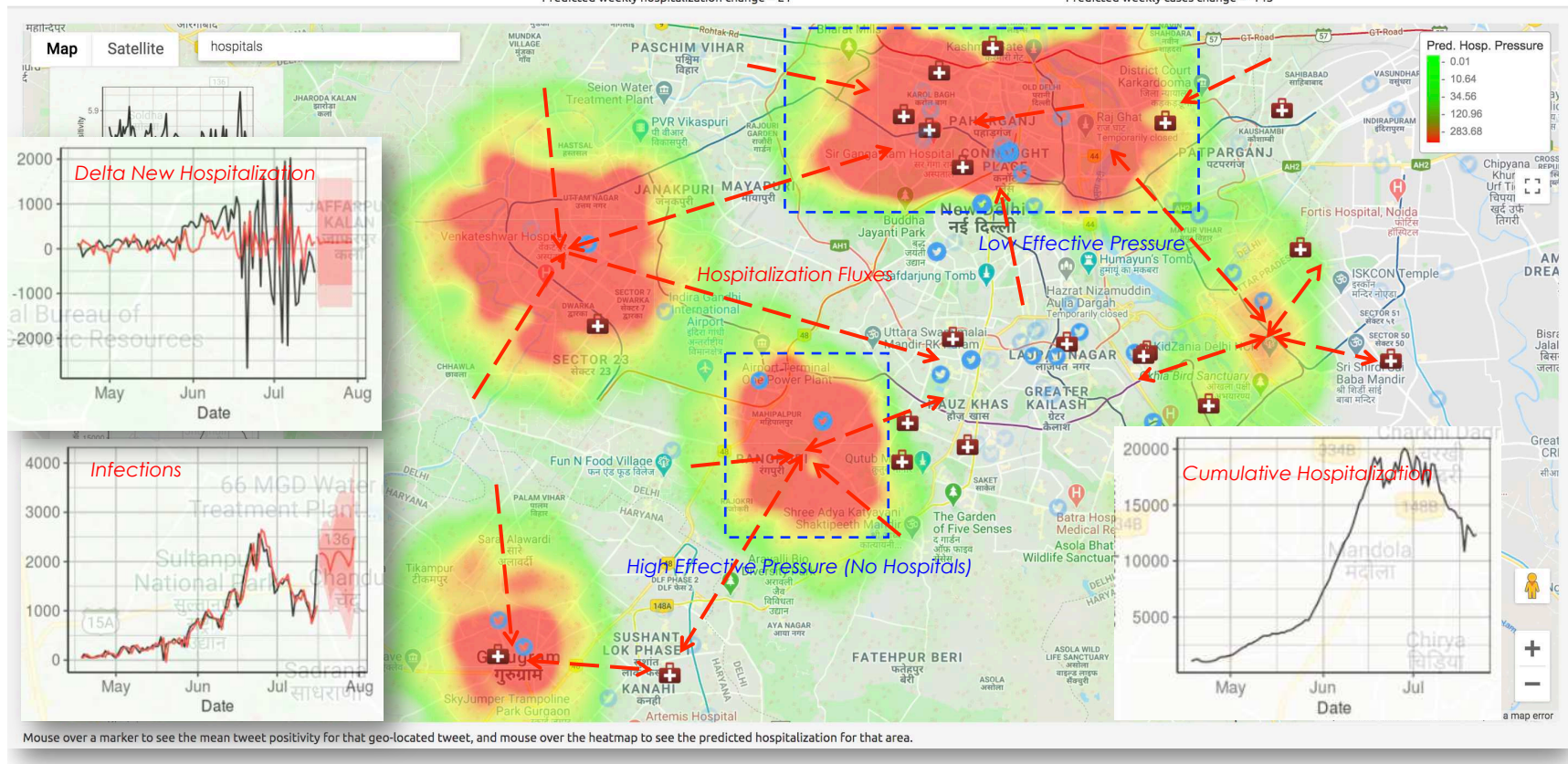
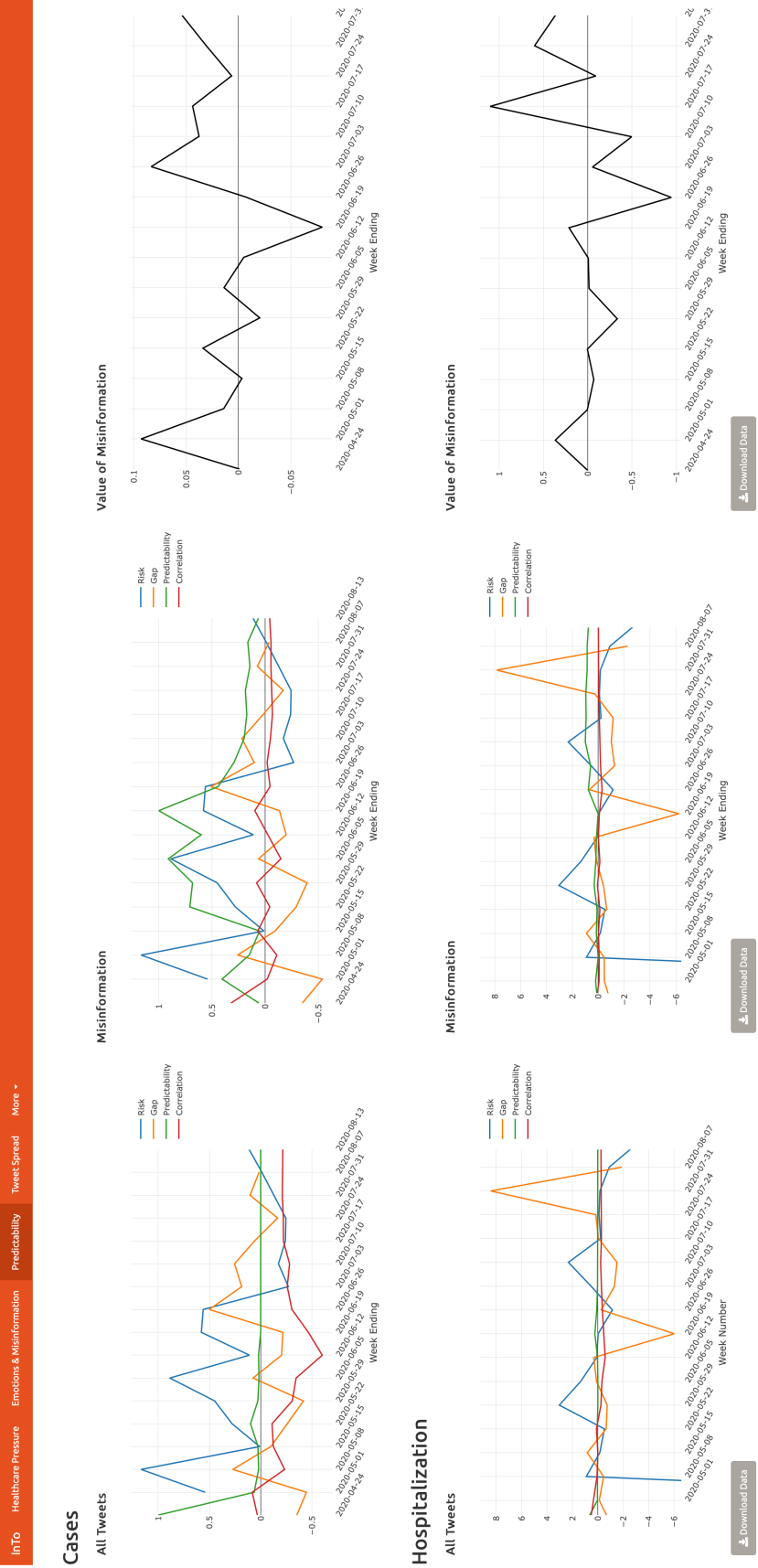


Figure 3:







Risk

Gap

Predictability

Correlation

2020-04-24

2020-05-01

2020-05-08

2020-05-15

2020-05-22

2020-05-29

2020-06-05

2020-06-12

2020-06-19

2020-06-26

2020-07-03

2020-07-10

2020-07-17

2020-07-24

2020-08-07

2020-08-13

Week Ending

Hospitalization

All Tweets

Misinformation

Value of Misinformation

Risk

Gap

Predictability

Correlation

2020-04-24

2020-05-01

2020-05-08

2020-05-15

2020-05-22

2020-05-29

2020-06-05

2020-06-12

2020-06-19

2020-06-26

2020-07-03

2020-07-10

2020-07-17

2020-07-24

2020-08-07

2020-08-13

Week Ending

Risk

Gap

Predictability

Correlation

2020-04-24

2020-05-01

2020-05-08

2020-05-15

2020-05-22

2020-05-29

2020-06-05

2020-06-12

2020-06-19

2020-06-26

2020-07-03

2020-07-10

2020-07-17

2020-07-24

2020-08-07

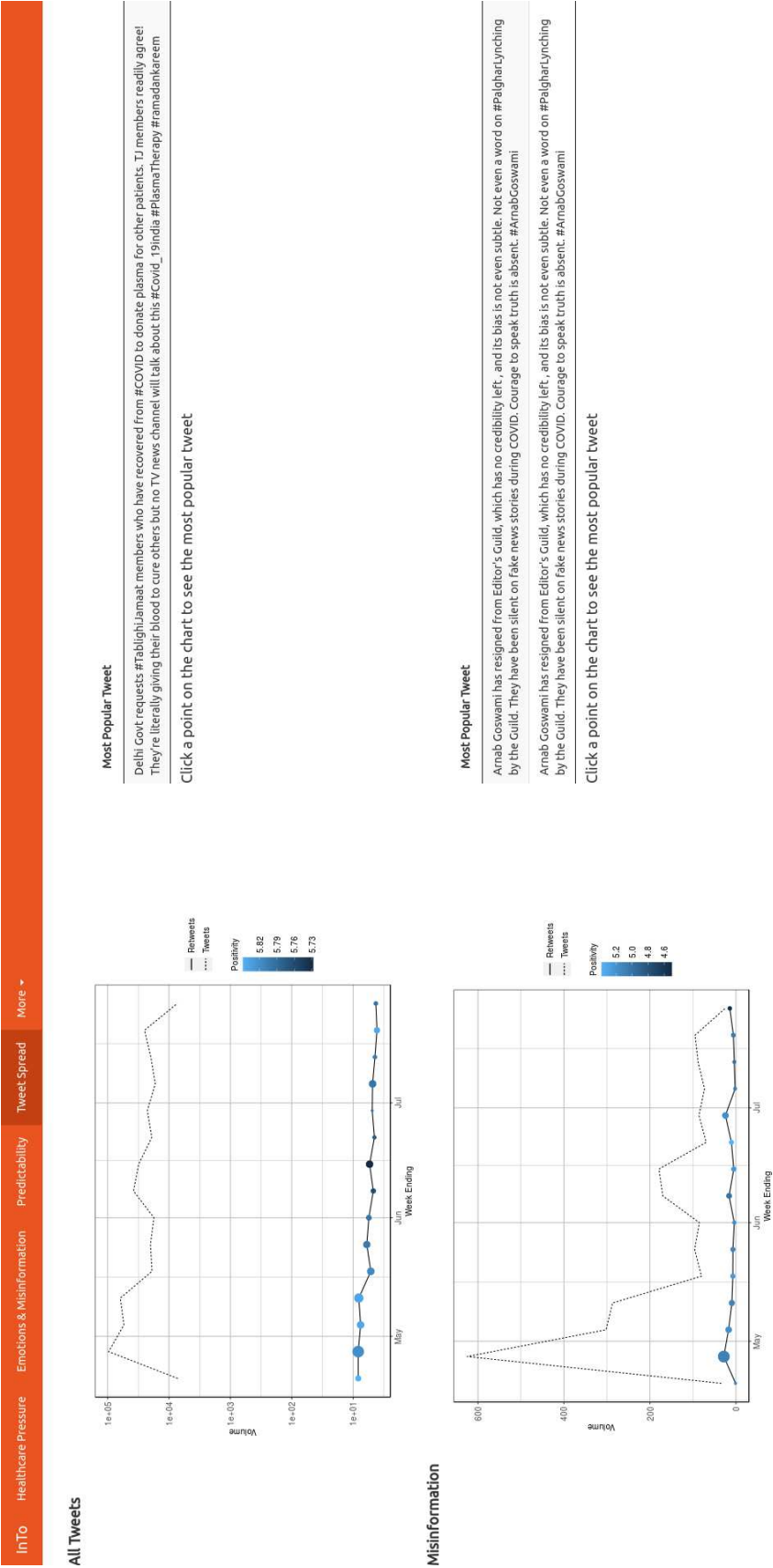
2020-08-13

Week Ending

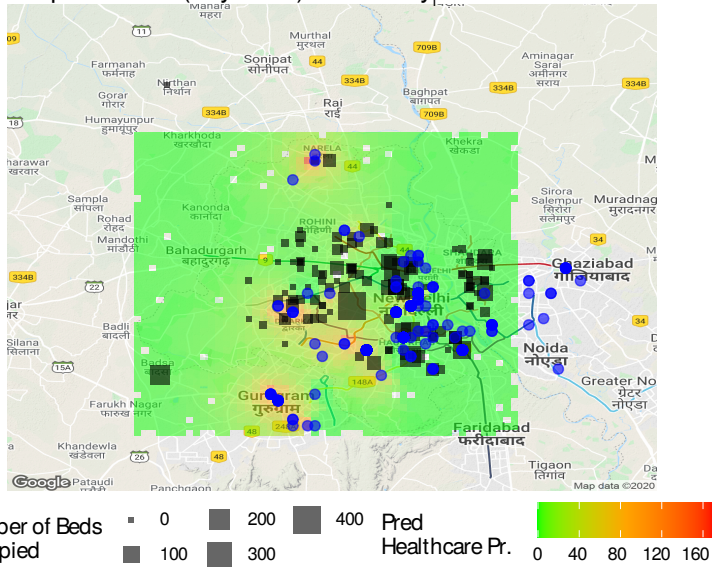
Download Data

Figure 5:

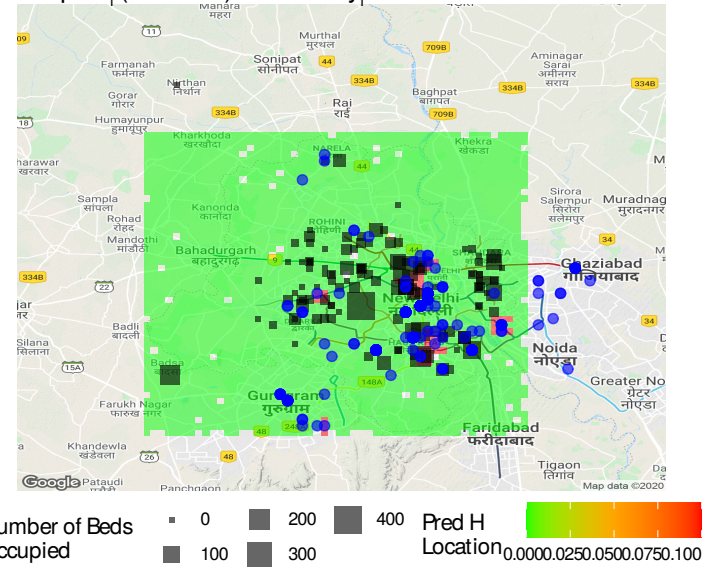




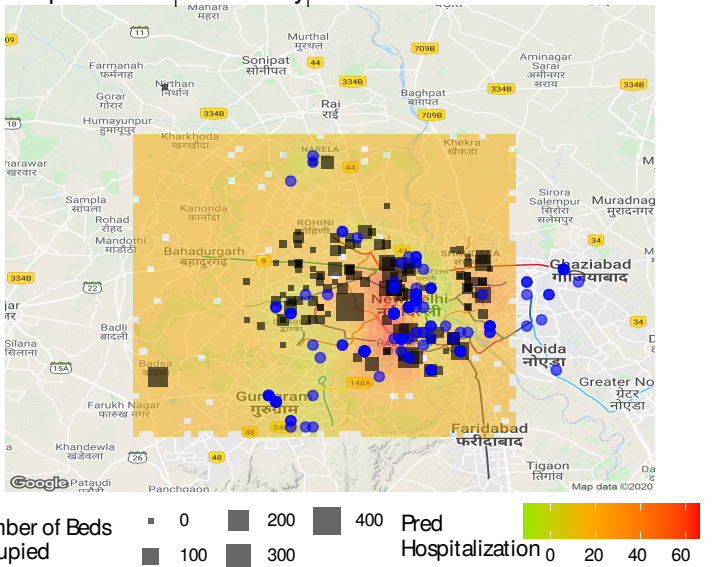
**A** Hospitalization (City Scale) ~ Positivity



**B** Hospital (Location) ~ Positivity



**C** Hospitalization<sub>i</sub> ~ Positivity<sub>i</sub>



**D** Hospitalization<sub>i</sub> ~ Hospital Bed Occupancy

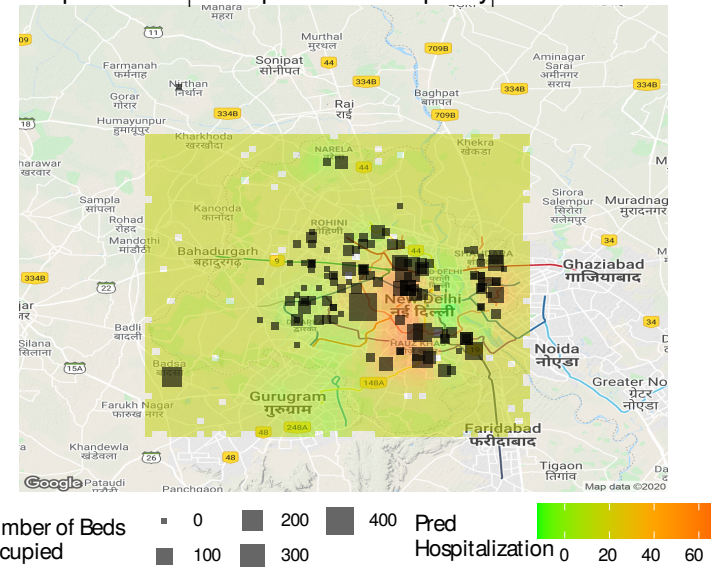


Figure 7:

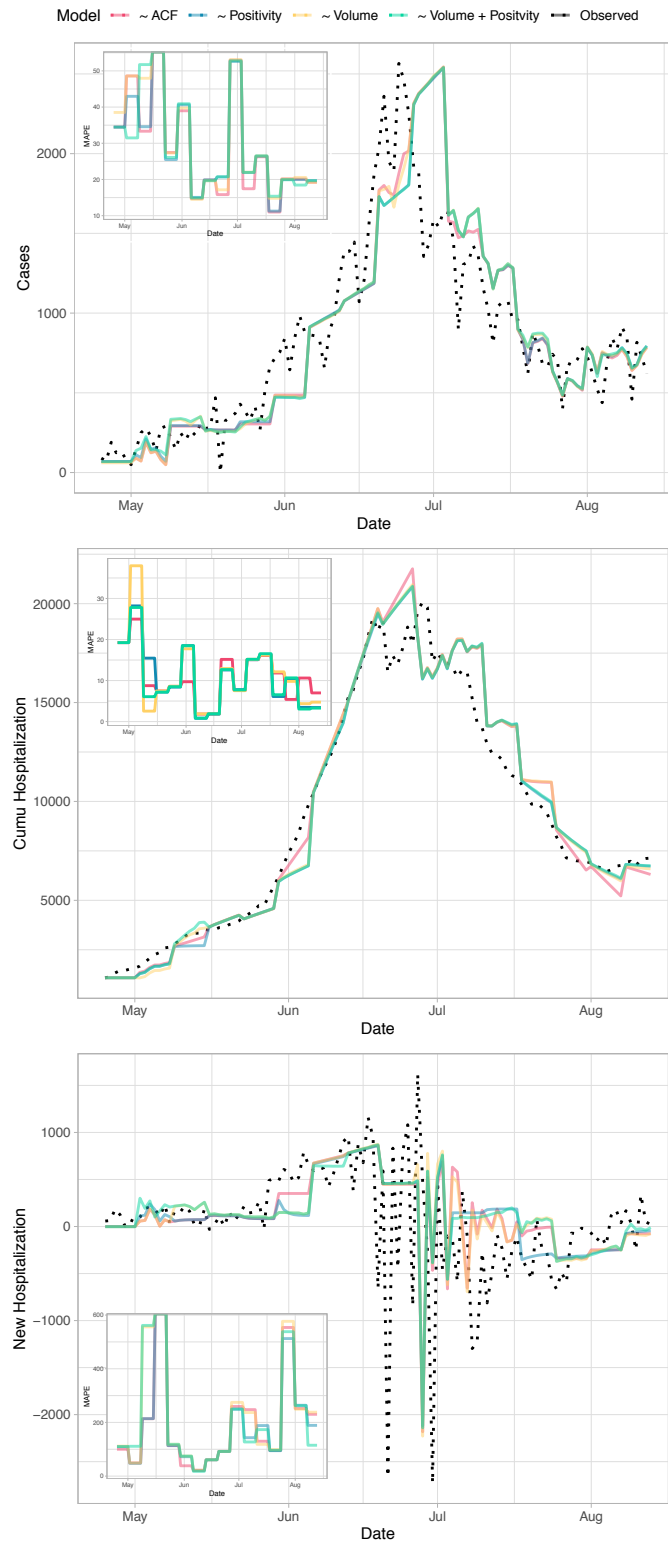


Figure 8: